Journal of Environmental Management 312 (2022) 114983

Contents lists available at ScienceDirect

Journal of Environmental Management

journal homepage: www.elsevier.com/locate/jenvman

Internal phosphorus loading and its driving factors in the dry period of Brazilian semiarid reservoirs

Maria de Jesus Delmiro Rocha, Iran Eduardo Lima Neto *

Department of Hydraulic and Environmental Engineering, Federal University of Ceará, FC, Bl. 713, Center of Technology, Fortaleza, Ceará, Brazil

ARTICLE INFO

Keywords:
Phosphorus. sediment release. wind speed. surrogates. eutrophication. reservoirs

ABSTRACT

This study investigated the relationships between physical, limnological and climatic drivers with the internal total phosphorus (TP) loading produced over the dry period in 30 water supply reservoirs of the Brazilian semiarid. Improvements in the understanding of sedimentary TP fluxes in reservoirs of dryland regions are pressing as they usually have serious water quality related issues, remaining mostly eutrophic especially under frequent drought events. Gross daily fluxes and net seasonal average release rates were calculated from mass balance and regression equations considering water and sediment TP concentrations, anoxic duration, water temperature and fish contribution. Additionally, the ratio of wind speed to reservoir volume was proposed as a new surrogate and then applied as explanatory variable to predictive models. The results indicated TP release rates higher than reported for non-semiarid lakes/reservoirs with average gross fluxes ranging from 17.64 to 35.99 mg m^{-2} day^{-1}. This may be attributed to the enriched sediments (1029.49 ± 552.49 mg kg^{-1}) allied with warmer water temperature, high trophic state, and prolonged anoxic periods (average duration of about 60 days). The average release rates were negatively correlated with water transparency and water depth, and positively correlated with Chl-a, wind speed and trophic state. The release rates increased across the trophic gradient ($p < 0.05$), about 10-fold higher under hypertrophic conditions than in oligotrophic ones. As anoxia is linked with eutrophication, phosphorus release is more likely in eutrophic ecosystems. Regarding the new surrogate, a strong predictive ability for TP release (R^2: 0.26–0.93) was observed. Similarly, the proposed models presented a physically consistent behavior with a stabilizing releasing pattern suggesting the achievement of equilibrium in nutrient exchange between sediment-water interface. This research advanced by combining and proposing methods to assess and quantify sedimentary fluxes in data-scarce regions balancing accuracy and transferability, in order to be replicable to other dryland environments globally.

1. Introduction

Understanding the role of sediment-water interactions and nutrient release from the sediment in reservoirs is a necessary step to assess important limnological processes (Wang et al., 2021). According to the history of phosphorus (P) pollution in a waterbody, the impact of the internal load can vary from nearly irrelevant to higher than the external inputs on an annual P budget (Orihe et al., 2017). The effect of the internal phosphorus loading can last for several years after significant reductions in external inputs delaying the recovery of waterbodies from poor water quality conditions (Katsev, 2017). Furthermore, even small release rates may cause significant disturbances in water column total phosphorus concentration (TP_w) (Horppila et al., 2017; Moura et al., 2020).

The internal P loading can be described as two different fluxes from sediment: a net internal loading rate and a gross phosphorus flux (Nürnberg et al., 2012). The net rate of P release is estimated through modeling, commonly by a whole-lake mass balance, representing the balance, on an annual or seasonal basis, between upward and downward flux of P from the water column (Barbosa et al., 2019). Contrastingly, the gross rates are the P rates directly released from sediment, which are usually measured from sediment incubation experiment (Orihe et al., 2017). As positive net rates are obtained, internal load is likely contributing to TP_w (Nikolai and Dzialowski, 2014).

The continuous accumulation and releasing of P from sediment results from several physical and biogeochemical mechanisms (Li et al., 2013; Katsev et al., 2006; North et al., 2015; Cavalcante et al., 2018; Tammeorg et al., 2020). More importantly, the relevance of the

* Corresponding author.
E-mail address: iran@deha.ufc.br (I.E. Lima Neto).

https://doi.org/10.1016/j.jenvman.2022.114983
Received 24 November 2021; Received in revised form 3 March 2022; Accepted 27 March 2022
Available online 4 April 2022

mechanisms driving internal P loading relies mainly on the time scale evaluated (Katsev et al., 2006; Markovic et al., 2019). To determine net retention or release rates on an annual or seasonal basis, short-term P fluxes from sediment may not be so relevant (Orihe et al., 2017). In that perspective, physical and environmental drivers are suitable to correlate and explain internal P loading in a long-term budget (Wang et al., 2015; Huang et al., 2021). They may also act as indicator surrogates more easily measurable to facilitate management goals (Hunter et al., 2016).

Physical aspects such as wind disturbance, inflow-outflow relationship, lake morphometry, mixing degree, light and water/ambient temperature strongly influence P dynamics (Håkanson, 2005; Matisoff and Carson, 2014; Zhang et al., 2016a,b; Liu et al., 2018; Huo et al., 2019). Additionally, data on climate and reservoir morphometry are strong predictors for P release and usually easier to access in comparison with sediment data (Zhang et al., 2017, 2020). The trophic state is another determining factor in sediment P release (Liu et al., 2018; Nürnberg et al., 2019). Hypereutrophic water bodies are more susceptible to present higher release rates than eutrophic or mesotrophic ones (Kowalczewska-Madura et al., 2015, 2019; Ostrofsky and Marbach, 2019). This is especially impactful in semiarid regions where eutrophication is a serious issue in drinking water reservoirs (Wiegand et al., 2021). Factors such as prolonged drought periods, irregular precipitation cycle and high evaporation rates incur great water losses and water level fluctuation (Santos et al., 2016a). Consequently, the reservoirs become shallower, eutrophic and vulnerable to internal loading effects (Freire et al., 2009; Coppens et al., 2016; Lira et al., 2020; Cavalcante et al., 2021).

The internal loading quantification in artificial reservoirs is a relatively new subject, less addressed than in natural lakes, especially in semiarid regions (Rocha and Lima Neto, 2021a; Lima Neto et al., 2022). However, in dryland regions reservoirs are strategic waterbodies which highlights the importance of these quantification in such environments (Noori et al., 2018, 2021a). Furthermore, lakes and reservoirs are inherently different regarding, among other aspects, the hydraulic residence time, the susceptibility to faster regime shifts, productivity level, anthropogenic usage in catchment and water level fluctuation (Noori et al., 2021b). The practice of aquaculture in reservoirs with fish-farming byproducts entering the limnetic environment is also an additional source upon the P budget (Johansson and Nordvarg, 2002; Santos et al., 2017). Combined, these factors differentiate the internal P loading estimation in reservoirs. Particularly in the Brazilian semiarid, over the past century a high-density reservoir network (one per about 5 km^2) has been built to provide human supply (Lima Neto et al., 2011). Then, allied with the aforementioned conditions, the water quality management of these reservoirs has become a major challenge.

Despite the internal loading relevance in these environments, efforts towards its quantification is still incipient, especially under sediment data scarcity (Nurnberg, 2009). Furthermore, as a detailed measurement of P exchanges in sediment-water interface (SWI) is very time and cost demanding and still a punctual representation of the phenomenon, an overall assessment of P release may be suitable as a first attempt of quantification. Then, to achieve a broader comprehension of the phenomenon in larger timescales, one may apply an approach that requires as few fitting parameters as possible (Katsev, 2017; Xu et al., 2020). Additionally, under resource constraints in monitoring the development of expeditious predictive models for sediment P release may assist with valuable support decision tools. The use of surrogates instead of in situ measurements is often necessary to achieve a cost-effective yet useful way to assess ecosystem responses and key ecological processes (Lindenmayer et al., 2015).

This research aimed to quantify the internal phosphorus load produced during the dry period and identify the most influencing factors on this loading in water supply reservoirs of the Brazilian semiarid. Specifically the goals were: (i) estimate gross release rates from sediment data and water quality parameters through regression approaches, (ii) estimate averaged net release rates from mass balance, (iii) statistically connect the net rates with single factors (P external fluxes, physical and environmental drivers, trophic state index) and coupling factors (mean lake level fluctuation and wind speed/volume ratio) and (iv) propose a new surrogate indicator to predict TP release rates. This work innovates in evaluating the internal P loading potential of semiarid reservoirs under data constraints while elucidating relevant driving factors affecting P release in dryland regions.

2. Methodology

2.1. Site description and reservoir selection

Thirty reservoirs located in the State of Ceará, Brazilian semiarid, were selected to carry this study. The selection considered, firstly, the strategic importance of the reservoirs into the network that supplies water for human, industrial, and agricultural uses in the state. Secondly, if the reservoir is under the continuous monitoring program of water quality, quantity, and catchment characterization of the Water Management Company of the State of Ceará (COGERH). The selection also covered morphologically different water bodies scattered over the state (Fig. 1) and captured a trophic-state gradient representative of the region as detailed in Table 1 with additional informations in Table S3. While most of the reservoirs are eutrophic ecosystems, copping measures to recover water quality are still incipient. Regarding water uses, priority is given to human supply and aquaculture. Concerning water-depth, Table 1 presents the maximum average depth ($\overline{H_{max}}$) measured at the dam of the reservoir during the dry period over the years 2010–2020. Ten reservoirs presented $\overline{H_{max}} \leq$10m and seven showed 10m$< \overline{H_{max}} \leq$12m. During the driest years (2013–2016) (See Fig. S5) the reservoirs became even shallower with seventeen presenting a $\overline{H_{max}}$ <10m (Table S3).

Due to the semiarid climate and the susceptibility to droughts, the water level, surface area, and water storage varies significantly. According to the Köppen classification, 90% of the State of Ceará is under a dry, hot semiarid climate with annual average temperature between 23° and 28 °C (Wiegand et al., 2021) and annual average evaporation rates of about 2 m yr^{-1} (Brazil, 2021). Summarizing important climatic aspects, semiarid reservoirs are under a high and relatively constant incidence of solar radiation, small seasonal variations in water temperature, wind influence and greater temperature variability occurring in a 24-h period (Souza Filho et al., 2006; Meireles et al., 2007; Dantas et al., 2011; Lemos, 2015; Lima Neto, 2019). Then, regarding the mixing regime, this aspects suggest that the study sites can be considered mostly polymictic reservoirs with a diurnal mixing cycle (up to 5 °C from bottom to top).

2.2. Data sources

COGERH provided the datasets of TP_w, water temperature (T), pH and dissolved oxygen (DO). The data was quarterly collected from in situ measurement using a multiparametric probe, previously calibrated with respective standard solutions, covering the ranges of values ordinarily recorded in the reservoirs. The laboratory analysis followed APHA (2005). During the dry period, the sampling frequency is usually in July/August and November/December and the sampling point is located near the reservoir's dam. Datasets on chlorophyll-a concentration (Chl-a) and Secchi depth (z_{secchi}) were also provided. Additional water surface data at 0.3 m deep of phosphorus ($TP_{surface}$), Chl-a and z_{secchi} was publicly available in Ceará (2021). A data consistency was performed to identify possible sampling errors. Data in other depths to provide a vertical profile of TP in the water column, however, was less frequent in the last four years and the available data have not achieved the deepest layers for most reservoirs. Despite limitations, the dataset of TP concentration in other depths provided important information on the temporal variability of vertical TP concentration. Additionally, it supported the

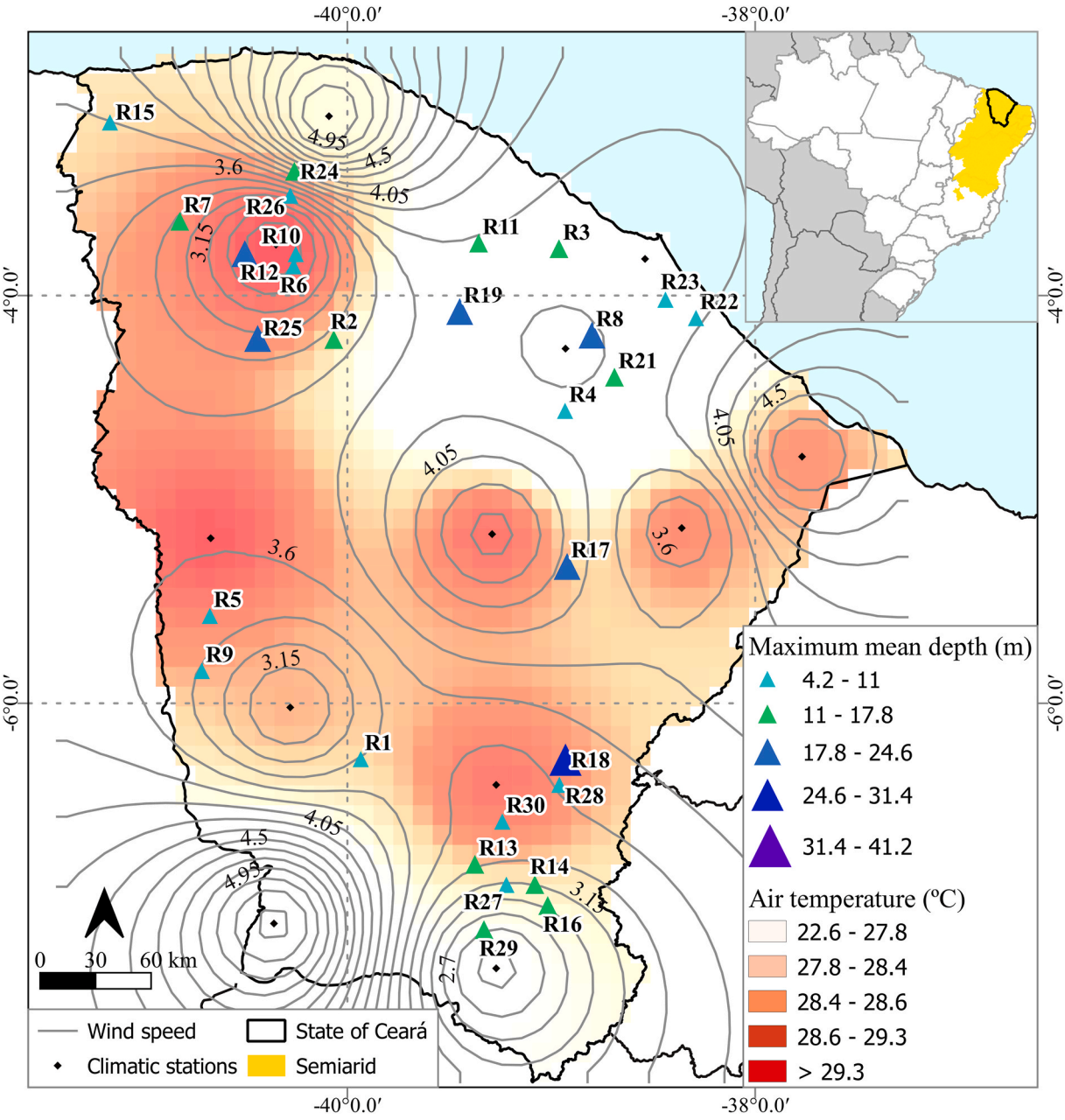

Fig. 1. Study sites and meteorological forcings in the State of Ceará, Brazil.

calculation of TP_w whenever possible.

Sediment measurements were performed in 2016 in the reservoirs R20 to R30 and were available in the environmental inventory of each one (Ceará, 2021). Total phosphorus (TPs), ion (Fe_s) and aluminium (Al_s) concentrations in the sediment were quantified. A detailed speciation of the P fractions was not available for the study sites. However, previous work in the study area and in other regions world-wide support the quantification of the internal loading as a mass of total phosphorus (Nurnberg, 2009; 2012, 2013; Rocha and Lima Neto, 2021a). Furthermore, although sediment measurement data were not performed in the remaining reservoirs, all reservoirs have a detailed quantification of the external TP load produced by their catchments, which was also used for model validation. The TP load contribution from the catchment is detailed in the supplementary material (Table S3 and Fig. S7).

The dataset of the trophic state index (TSI) of the reservoirs was also available in Ceará (2021). TSI was calculated from TP_w, z_{secchi} and Chl-a through the method proposed by Toledo et al. (1983). This method has been adapted considering specific characteristic of tropical systems, such as the low water transparency due to the high mineral turbidity (Lima Neto et al., 2011; Klippel et al., 2020). The datasets comprised the period of 2008–2020. Data related with reservoir morphometry and operation (volume, water level, surface area and released flow) were obtained from Ceará (2021). The climatic characterization was performed from twelve climatological stations scattered across the study area (see Fig. 1). The climatic variables were obtained from the nearest station of each reservoir. The dataset covers a thirty-years monitoring period (1981–2010) of the National Meteorological Institute to settle representative monthly averages to each station. The wind intensity was measured by an anemometer at 10 m high (Brazil, 2021).

2.3. Internal load modeling

2.3.1. Assumption for fish contribution

Fish farm emissions may be accepted as a fast-sinking particulate

Table 1
Physical characterization of the reservoirs and water quality conditions.

ID	Water surface area (km^2)[a]	Maximum mean depth (m)[a]	Reservoir age[b]	Miminum surface TP concentration (mg L^{-1})[a]	Average surface TP concentration (mg L^{-1})[a]	Maximum surface TP concentration (mg L^{-1})[a]	Representative trophic state[c]
R1	1.5	8.9	55	0.010	0.124	0.417	Eutrophic
R2	13.8	17.5	34	0.010	0.081	0.145	Eutrophic
R3	15.6	10.2	22	0.033	0.158	0.453	Eutrophic
R4	1.7	7.3	24	0.044	0.154	0.442	Eutrophic
R5	5.0	6.4	22	0.026	0.175	0.574	Eutrophic
R6	2.3	9.4	29	0.022	0.059	0.107	Oligotrophic
R7	7.3	12.1	23	0.015	0.051	0.194	Eutrophic
R8	1.6	18.3	97	0.010	0.111	0.285	Eutrophic
R9	1.0	7.1	23	0.044	0.120	0.599	Eutrophic
R10	4.9	9.1	94	0.021	0.092	0.347	Eutrophic
R11	8.5	12.0	59	0.032	0.075	0.206	Eutrophic
R12	7.8	19.6	85	0.037	0.079	0.142	Eutrophic
R13	1.3	11.7	23	0.010	0.042	0.278	Eutrophic
R14	4.9	15.1	20	0.010	0.052	0.475	Eutrophic
R15	12.6	8.0	20	0.014	0.038	0.089	Eutrophic
R16	2.6	14.5	21	0.010	0.041	0.118	Mesotrophic
R17	37.2	29.3	55	0.046	0.122	0.280	Eutrophic
R18	79.8	28.4	60	0.010	0.080	0.142	Eutrophic
R19	10.3	18.3	86	0.010	0.109	0.473	Mesotrophic
R20	162.5	41.2	18	0.015	0.103	0.219	Eutrophic
R21	7.5	17.1	18	0.026	0.056	0.112	Eutrophic
R22	4.0	10.8	18	0.027	0.179	0.364	Eutrophic
R23	2.6	7.9	19	0.040	0.169	0.431	Eutrophic
R24	1.2	11.7	98	0.023	0.044	0.072	Eutrophic
R25	20.1	24.2	63	0.025	0.091	0.183	Eutrophic
R26	4.7	10.2	114	0.015	0.045	0.073	Oligotrophic
R27	0.3	4.2	63	0.020	0.101	0.354	Eutrophic
R28	6.7	7.7	97	0.031	0.100	0.208	Eutrophic
R29	1.0	19.6	36	0.014	0.058	0.230	Mesotrophic
R30	3.4	10.3	22	0.023	0.058	0.104	Eutrophic

[a] From measurements taken during the dry period (01/jul – 31/dez) in the study period (2008–2020).
[b] From the year of conclusion of the construction to 2021.
[c] Calculated from how many times the TSI was attributed to the reservoir over the total number of TSI classifications in the study period (2008–2020). For each field campaign carried out by COGERH a TSI is attributed to the reservoirs.

fraction which in a short-term mass balance is momentarily transported to the sediment (Johansson and Nordvarg, 2002). However, in a long-term perspective, the origin of the P released fraction might be difficult to track, especially the undercage release (Kelly, 1993). In this study, nine reservoirs with aquaculture practice were incorporated among the study sites. This was necessary in order to not exclude of the study the largest and more strategic reservoirs of the state (R18 and R20) (Ceará. Bureau, 2018). Based on this criteria, reservoirs R18, R20 and the remaining medium-sized and small reservoirs with such practice were considered. Furthermore, the study of reservoirs through an approach that separate the load of the aquaculture from the seasonal budget is an alternative. On the contrary, the study of the internal P loading in such waterbodies would be neglected in face of the difficulty to address the aquaculture contribution.

To quantify the TP load from aquaculture was necessary to separate fish contribution. This quantification involved the delimitation of the area of fish cages, farming productivity, P concentration in the fish feed and the coefficients related with feed conversion and apparent digestibility. Detailed information on the P load from aquaculture and the estimation process is presented in Ceará (2021). Then, to perform the P budget in this study, the fish contribution was assumed to be constant over the years, equal to the field estimate reported by COGERH and was deducted from the modeled P load following the methodology proposed by Nürnberg et al. (2012). Although this estimate may not precisely relate to specific years, it attempted to remove the average fish contribution from the seasonal balance when performing the budget (Nürnberg et al., 2012).

2.3.2. Phosphorus budget for net internal load

The dry period of the Brazilian Northeast is characterized from mid-June to December, covering the seasons Winter and Spring with negligible precipitation indexes (Costa et al., 2020). Therefore, irrelevant rainfall-related inflow to the reservoirs is expected. Furthermore, due to the shallow soils over crystalline rocks, base flow is also negligible, while the rivers are intermittent (Ceará, 2021). Under these conditions is possible to quantify with less interference possible the actual internal load. Eq. (1) presents the one-box mass balance model proposed by Vollenweider (1968) applied to estimate the average net P loading from TP_w. As the elapsed time between TP measurements covers the dry period, the modeled load is assumed to represent the averaged net internal TP load produced over this period. The average TP_w was used whenever available water samples in other depths. When not, the surface concentration was used assuming a complete-mixed behavior (Rocha and Lima Neto, 2021a). The results supporting this hypothesis are presented and discussed in results section.

$$TP_w(t) = TP_{w,0}.\exp\left(-\left(\frac{Q_s}{V}+\frac{4}{\sqrt{RT}}\right).t\right) + \left[L \Big/ \left(Q_s + \frac{4}{\sqrt{RT}}V\right)\right].\left[1-\exp\left(-\left(\frac{Q_s}{V}+\frac{4}{\sqrt{RT}}\right)t\right)\right] \quad (1)$$

where $TP_w(t)$: TP concentration at the reservoir outlet at a given time (kg m^{-3}); $TP_{w,o}$: Initial TP concentration (kg m^{-3}); t: Elapsed time (month); V: Average reservoir volume (m^3); L: TP load (kg $month^{-1}$); Q_s: Released flow (m^3 $month^{-1}$); RT: Theoretical hydraulic residence time ($month^{-1}$).

The settling loss rate $\left(\frac{4}{\sqrt{RT}}\right)$ is an empirical model validated for semiarid reservoirs (Lima, 2016; Araújo et al., 2019; Toné and Lima Neto, 2019; Rocha and Lima Neto, 2021b; Lima Neto et al., 2022) while the RT was calculated as proposed by Rocha and Lima Neto (2021a) for the dry period of dryland regions. Ultimately, the net areal P loading (L_net) was calculated by the ratio $L.A^{-1}$, where A is the mean lake

surface area of the period. As the unit representation for this estimate varies widely in the literature depending on the study period (mg m^{-2} $summer^{-1}$, mg m^{-2} $season^{-1}$, mg m^{-2} $Aug\text{-}Sep^{-1}$, mg m^{-2} yr^{-1}) (Nürnberg et al., 2019), in this work a new unit representation (mg m^{-2} dry $period^{-1}$) was adopted to accurately describe the particularity of tropical semiarid regions.

2.3.3. Gross sediment fluxes and active sediment release factor

The gross internal P loading (L_gross) in shallow lakes may be estimated from the product of the gross fluxes of P release (RR in mg m^{-2} day^{-1}) by the actively releasing area of the sediment modeled as the anoxic factor (AF in day per dry period) (Nürnberg, 2005). In this work, the definition of anoxia (DO < 2 mg L^{-1}) and hypoxia (3–5 mg L^{-1} DO) follows Nürnberg (2019). L_gross was estimated for the dry season of the years in the study period in which there was available data. To obtain RR, the literature provides several predictive models validated in different regions world-wide. These models apply different variables, such as sediment TP concentration (TP_s) or lake water quality data. For this work, as TP_s was available for 37% of the reservoirs, four different models were tested to estimate RR: Eq. (2) (Nurnberg et al., 1986), 3 (Carter and Dzialowski, 2012), 4 (Moura et al., 2020b), 5 (Cheng et al., 2020) and 6 (Chapra and Canale, 1991; Lira et al., 2020). Eq. (6) requires TP_s while the remaining methods attempted to correlate RR with water quality data or other physical parameters.

$$RR_1 = 12.116 \cdot \log(TP_w) - 9.708 \quad (2)$$

$$RR_2 = 10^{\hat{}}\left[-0.54 + 0.827 \cdot \log\left(TP_{surface}\right)\right] \quad (3)$$

$$RR_3 = 0.3332 \cdot Age \quad (4)$$

$$RR_4 = 1.0482 \cdot RR_1 \cdot \exp[0.099 \cdot (T - 20)] \quad (5)$$

$$RR_5 = v_r \cdot \rho_s \cdot TP_s \quad (6)$$

where RR: TP release rate (mg m^{-2} day^{-1}); ρ_s: Dry-bulk density (kg m^{-3}); v_r: coefficient of phosphorus recycled mass-transfer from sediments to the water (m day^{-1}); Age: Reservoir age (yr); T: Water temperature (°C).

Eq. (2) was developed for temperate lakes and was applied combined with Eq. (5). Eq. (5) was developed experimentally considering a flowing overlying water with low velocity plus static sediments. Eq. (5) also considers a correction of RR from estimates at 20 °C to any arbitrary temperature, which is a relevant aspect as Brazilian water bodies have higher water temperatures (~30 °C). For the model presented in Eq. (3), although developed for temperate lakes, is necessary only $TP_{surface}$ data, which is largely available in the study sites and turns it the most practical model to apply. Eq. (4) was designed with data of semiarid reservoirs to estimate RR from reservoir age. In Eq. (6) the parameter v_r applied was calibrated by Lira et al. (2020) ($v_r = 0.00097$ m $month^{-1}$) to a reservoir located in the study region. This value was also very close to the that reported by Chapra and Canale (1991) (v_r = 0.00096 m $month^{-1}$).

Assuming that Eq. (6) results the most accurate estimates since is applied sediment data, the Pearson correlation coefficient (r^2), the Mean absolute percental error (MAPE) between the medians, and the relative index of agreement (r_d) were evaluated to validate the release rates. The relative index of agreement was developed by Willmott (1981) to overcome the insensitivity of correlation-based measures. The r_d was calculated as presented in Eq. (7) for each method described from Eq. (2) to Eq. (5) considering RR_5 and the median of the respective method for the reservoirs R20-R30. These reservoirs were considered as there was available measured sediment data. Then, the model with the best metrics was applied to calculate L_gross for all reservoirs.

$$r_{d,j} = 1 - \frac{\sum_{i=1}^{11}\left(\frac{RR_{5,j} - RR_{j,i}}{RR_{5,i}}\right)^2}{\sum_{i=1}^{11}\left(\frac{\left|RR_{j,i} - \overline{RR_5}\right| + \left|RR_{5,i} - \overline{RR_5}\right|}{\overline{RR_5}}\right)^2} \quad (7)$$

where $r_{d,j}$: Relative index of agreement of the method j; $RR_{5,i}$: TP release rate of the ith reservoir estimated by Eq. (6) (mg m^{-2} day^{-1}); $RR_{j,i}$: TP release rate of the ith reservoir estimated by the method j (mg m^{-2} day^{-1}); $\overline{RR_5}$: Average RR_5 estimates considering all reservoirs (R20-R30).

Eq. (8) describes AF as proposed by Nürnberg (1995). AF is one of the several ways to quantify oxygen depletion chosen in accordance with the available data. The objective is to quantify the spread and duration of anoxia or hypoxia events. The AF is a ratio that represents the number of days in a period that a sediment area equal to the lake or reservoir surface area is anoxic or hypoxic (Nürnberg, 2019). AF is predictable from TP_w and reservoir morphometric data considering that the actively P releasing area may not be restricted to those overlain by anoxic water, especially in polymictic lakes (Nürnberg, 2019). The unit is commonly expressed as day per summer or day per season which was adapted here as day per dry period (day dry $period^{-1}$). This equation has already been validated to eutrophic shallow and mixed lakes (Nurnberg, 2009) and applied to lakes world-wide including arid and semiarid environments (Townsend, 1999; Kiani et al., 2020; Lima Neto et al., 2022; Tammeorg et al., 2020).

$$AF = -36.2 + 50.1 \;\; Log(TP_w) + 0.762 \;\; x\frac{Z}{A^{0.5}} \quad (8)$$

where TP_w: Average concentration in the water column during the period (μg L^{-1}); Z: Lake mean depth (m); A: Lake surface area (km^2).

2.4. Driving factors on P release rates

2.4.1. Surrogates for climatic factors

The variables wind speed, insolation and air temperature were selected as surrogates for climatic factors that potentially influence the internal loading. The paired dataset encompassing all reservoirs of RR and the respective average climatic variable calculated for the same period of the RR estimate was divided in subsets according to three ranges predefined for each variable. Then, to assess significant differences in RR depending on the ranges of the environmental variables, pairwise statistical analyses were performed by the Kruskal-Wallis (K–W) and Mann-Whitney (M-W) tests considering a significance level $\alpha = 0.05$ (Cleophas and Zwinderman, 2016). The null hypothesis considers RR independent of the magnitude of the environmental variable. Additionally, box plots were presented with the adopted thresholds beyond which RR might be significantly affected.

2.4.2. Trophic state and lake level influence

Analyzing the influence of the trophic state followed similar approach of the climatic surrogates aforementioned. To test for differences in P release rates among trophic states, the grouped datasets encompassing the release rates of all reservoirs by trophic state type were statistically analyzed with the K–W and M-W tests. The unequal length of observations within each subset favored the application of this non-parametric tests. The statistical tests were also performed for each reservoir. However, as the reservoirs remained with one trophy level for most part of the study period (see Table 1), they presented short subsets for the non-representative trophic state type which turns the results on the single reservoir level less reliable. An algorithm in Python language was designed in order to test each group against all the other groups. Then, post-hoc tests were not necessary.

The behavior of P release rate over time and its relationship with the level variation was additionally evaluated. The fluctuation in the reservoir's level intends to evaluate the long-term interannual stability of a

system, the average strength of the seasonal fluctuation and may also serve as a proxy for bottom-up driven processes (Kolding and van Zwieten, 2012). Then, the ratio between the daily lake level and half of the maximum depth of the respective dry period of each year was calculated. This indicator range from 0 to 2 and visually helped to evaluate the reservoirs drying up and this impact on P release.

2.5. Predictive model for internal P loading

Previous studies have attempted to use several lake morphometric characteristics combined as predictors for internal P loading (Tammeorg et al., 2017, 2020). Others have already applied combinations of morphometric and environmental characteristics, such as the ratio of wind speed to lake depth (Håkanson, 2005; Zhang et al., 2017; Jalil et al., 2019; Huang et al., 2021). In this study, the P release rate was logarithmically correlated with the wind speed to reservoir volume ratio for each lake. The ratio of wind speed to mean reservoir volume was adopted here as a suitable surrogate. Firstly, because the effect of wind-induced shear stress to enhance the advection-diffusion transport of chemicals across SWI is considered. Secondly, this surrogate considers the influence of the volume in the stability, productivity and increasing in nutrient concentration of the reservoir (Gownaris et al., 2018). The coupling of these variables turns into a potential indicator to explain the release process (Hunter et al., 2016). For each statistical model adjusted, the goodness of fit was evaluated through the metrics coefficient of determination (r^2), adjusted coefficient of determination (r_a^2) and the Mean Absolute Percentual Error (MAPE). Additionally, the analysis of the homoscedasticity of the model residuals was performed graphically assessing whether the residuals fit linear, quadratic or exponential curves.

2.6. Uncertainty, sensitivity analysis and model validation

Data accuracy and an outlier analysis were performed followed by removal of non-specific values below the detection limit (TP $<$ 0.01 mg L^{-1}). Additionally, a sensitivity analysis to identify the impact of the modeling most influencing parameters was performed as descripted by Rocha and Lima Neto (2021a). The volume and the difference in TP_w between the elapsed time in the modeling interval ($TP_{w,t}/TP_{w,0}$ ratio) more strongly influenced the results. Then, an analysis on these parameters was performed in light of the threshold reported by the above-mentioned authors. The coefficient of variation of the estimated loads was calculated and compared with others reported in literature to assess the model variability. Moreover, since the complete mix hypothesis is commonly accepted for the reservoirs in the study region as already presented (Lima Neto et al., 2022), eventual statistically significant differences between $TP_{surface}$ and those measured in other depths were assessed for each reservoir by K–W and M-W tests (α = 0.05).

2.6.1. Comparison with gross external P loading

The study sites present an environmental inventory elaborated by COGERH, which estimated the gross external TP load according to the Export Coefficient Modeling (ECM) approach (Ceará, 2021). The main external TP sources (agriculture, livestock, soil, sewer and aquaculture) in an annual timestep (t yr^{-1}) were accounted. Therefore, in order to assess and reinforce the order of magnitude of the estimated internal P loads, they were compared with the external load excluding fish contribution (L_ext). To keep consistency between units, gross, net and external loads were converted to a monthly average (t $month^{-1}$).

3. Results and discussion

3.1. Water quality characterization

3.1.1. TP and DO variation among and within reservoirs

Filled contour plots with polynomial smoothing based on TP and DO concentration profiles indicate the mixing status regarding these nutrients in the study sites from 2009 to 2019 (Fig. 2). The hatched area limits anoxic waters (DO $<$ 2 mg L^{-1}). The reservoirs in Fig. 2 were selected to cover from the shallowest to the deepest one. However, the profiles for all reservoirs along with pH and water temperature plots are available in the supplementary material. For most reservoirs, increasing TP_w has been noted during the driest years (2013–2016) (Jepson et al., 2021). As expected, water quality rapidly deteriorates under drought events (Cavalcante et al., 2021; Zou et al., 2020). At the end of 2016, eighteen reservoirs were below 10% of the maximum capacity and twenty-four below 20%.

The variation in TP_w among reservoirs is remarkable. R15 presented the lowest average concentrations (0.02–0.09 mg L^{-1}) while R9 presented the highest ones (0.06–0.90 mg L^{-1}). Accordingly, R15 presented the highest DO values while R9 presented the lowest ones. In average, the concentration considering all reservoirs was about 0.11 mg L^{-1} ($\pm$0.12) which is within the ranges reported in literature for eutrophic ecosystems. Huo et al. (2019) found a limiting TP concentration as a threaten criterion for Chinese lakes as 0.021 mg L^{-1}, which is about 6-fold lower than the observed values in the study sites. Uncommonly high TP concentrations ($>$4 mg L^{-1}) were excluded as probable measurement errors considering that the TP concentration in sewer is about 4 mg L^{-1} (Sperling, 2007). Eventual peak values (1–4 mg L^{-1}) were observed in R20 in 2016, when the reservoir was with a very low volume, and in reservoirs R9, R11, R18, R19 in 2009–2010, which was after the last strong rainy season of the past twelve years (Jepson et al., 2021). As influencing factors in the inter-reservoir variation may be highlighted the size and form (Håkanson, 2005), variable water retention time (Chaves et al., 2013), evaporation rates, volume variation and drought response (Coppens et al., 2016), inflow and input load during the prior wet period (Rattan et al., 2017), aquaculture practice (Gurgel-Lourenço et al., 2015) and climatic forcings (Zhang et al., 2020).

A marked interaction between surface and bottom TP concentration was observed in reservoirs R17 and R18. R18 presented high concentrations in the deeper layers from 2016 that lasted and increased while the water-depth reduced. This high concentration also spread to upper layers (See Fig. 2). Accordingly, DO concentration decreased from 2016 remaining under 2 mg L^{-1} from then on. In 2019 anoxic conditions (DO $<$ 2 mg L^{-1}) were observed even in the surface layers. High TP concentration in deep layers under anoxic conditions is a strong indicator of internal loading effect (Lopes et al., 2014; Andrade et al., 2020). Internal P loading may account for about 54% in TP_w increase (Ding et al., 2018). Studies suggest that deep-water hypoxia frequently develops in SWI of eutrophic ecosystems and is accelerated in warmer climates (Fukushima et al., 2017). Furthermore, the deeper layers may remain anoxic favoring P release even after the reservoir began to mix (Nikolai and Dzialowski, 2014). During the pre-drought years, high water depth may act as a protective mechanism trapping P in deep layers (Kowalczewska-Madura et al., 2019b). However, as the reservoir became shallower, short-term changes may also be influenced by wind shear and wave action potentially contributing to this P increase (Lepori and Roberts, 2017).

The behavior observed in R20 with simultaneously high concentrations in surface and deep layers with a transition zone between these layers may be influenced by factors such as aquaculture presence and anoxic/hypoxic events which widely occurred in the study period (See Fig. 2). Moreover, this reservoir has a strong fish farming production which might have contributed to sediment enrichment, high concentrations in the upper layers, and, combined with the water velocity, the dispersion of related pollutants in a broader area around fishcages

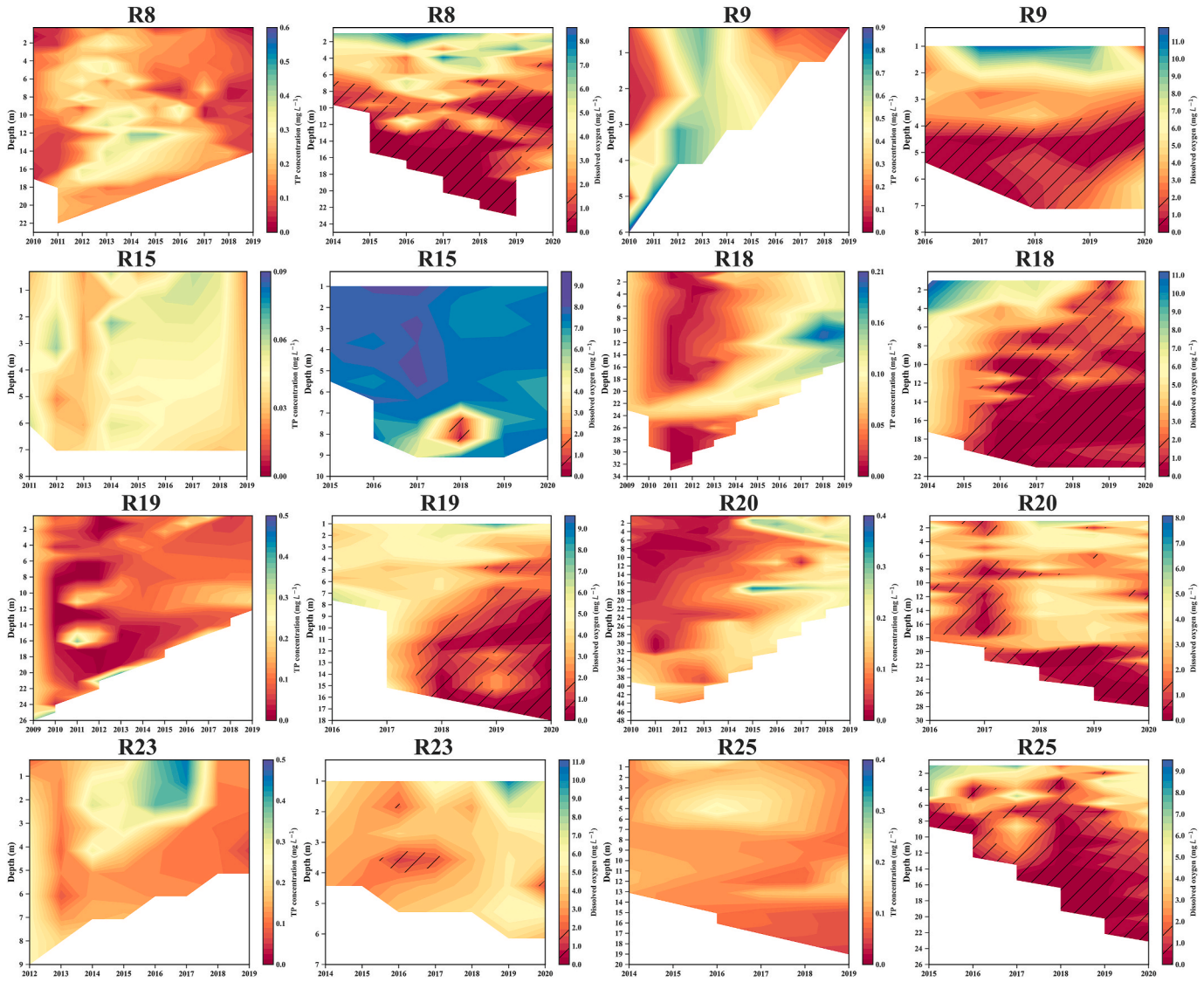

Fig. 2. Contour plots for the vertical profile of TP and DO concentration over the period of available data in the study period of 2008–2020. Measurements quarterly collected in the sampling point near the dam of the reservoir.

(Molisani et al., 2015; Lacerda et al., 2018). Additionally, the results reported by Molisani et al. (2015) highlighted that the external sources still induce worst water quality conditions than aquaculture. In fact, the L_ext of this reservoir is about 600 t yr^{-1} (Ceará, 2021).

Reservoirs R9 and R15 presented a markedly mixed vertical profile of TP concentration, mainly during 2012–2015. The worst condition was observed in R9, the shallowest reservoir, with average TP_w around 0.52 mg L^{-1} (±0.25). Shallow waterbodies and also the littoral zone of deeper lakes are more susceptible to wind-induced water column mixing and increasing nutrient concentration driven by resuspension (Cyr et al., 2009). Furthermore, as low DO concentration was observed, despite the low depth, not only physical releasing processes might have occurred. Even in shallow reservoirs under aerobic conditions (R15), significant amounts of P may be released driven by turbulence. The turbulence induces mixing and an increase in the in-lake flow velocity, which may cause a gradient of phosphate concentration at the SWI increasing P release (Kowalczewska-Madura et al., 2019b). Additionally, warmer SWI adequately oxygenated might favor microbially-mediated mineralization of organic P (Nicholls, 1999).

Regarding the vertical pattern and mixing status of the TP concentration and its variation over the study period (See Fig. 2 and Fig. S1), one can first highlight the impact of depth on the differentiation between concentrations in the deeper and surface layers. Only by evaluating these figures, it can be observed that the reservoirs with a depth less than 20 m showed similar concentrations throughout the vertical profile during the study period. The result of the statistical tests performed between TP measurements in the surface and in other depths revealed no significant differences in 70% of the reservoirs at a 95% confidence level. Part of the reservoirs with significant differences were also those with a more unbalanced dataset towards surface measurements, which might have biased the results.

However, in reservoirs with depths greater than 20 m (R8, 11, 17, 18 and 20), the greater depth combined with a low DO concentration (See Fig. S2) potentially favored events of phosphorus release from the sediment. Meantime, due to the depth, the high concentrations remained in the deeper layers. When these reservoirs became shallower (See R17, 18, 20 in Fig. 2), these high concentrations at the bottom spread to the entire water column, highlighting an intense mixing process at lower depths. Overall, the mixing pattern observed in the study sites may be driven by several factors such as the increasing wind forcing effect and the temperature impact on DO concentration as the reservoirs become shallower (Santos et al., 2016; Katsev, 2017).

3.1.2. Water transparency and chlorophyll-a concentration

Fig. 3a synthesizes the parameters Chl-a, $TP_{surface}$ and z_{secchi} for all study sites plotted against the water depth in the day of the sample collection along with the grouped data of z_{secchi} (Fig. 3b) and Chl-a concentration (Fig. 3c) by year. Chl-a and $TP_{surface}$ were negatively correlated with water depth as z_{secchi} was positively correlated as expected (Carneiro et al., 2014). Chl-a values reached 0.69 mg L^{-1} with average of 0.048 mg L^{-1}. For z_{secchi}, the values ranged from 0.1 to 4.20 m with average of 0.99 m. Consistently, the reservoirs with the highest z_{secchi} values were those with better water quality conditions. As for the temporal pattern, in 2009 the average z_{secchi} was about 1.5 m. This average value decreased continuously until 2014 when reached 0.5 m. From 2014 to 2016 the average z_{secchi} remained stable around 0.5 m. Then, from 2017 an increase in this average was observed reaching 1.0 m in 2020. Chl-a average values also responded over time on a similar trend as z_{secchi}, but with an inverse behavior.

These water quality surrogates presented a consistent pattern in response to the water level variation of the reservoirs over the study period, representing a continuous water quality degradation of these environments. As the reservoirs became shallower over the years, they also became particularly susceptible to wind action, resuspension of bottom sediments and reduction in water transparency, especially during the dry period (Freire et al., 2009). Accordingly, Chl-a concentration tends to increase with increasing wind speed and air temperature (Huang et al., 2021; Stefanidis et al., 2021). From analyzing the grouped dataset of TP_w by month, more frequent high measurements (0.20–0.40 mg L^{-1}) were observed at the end of the dry period. Similarly, peak Chl-a values were also more frequent at the end of the dry period, and, as shown in Fig. 3, in the years 2014–2016. In the recent literature several predictive models for internal P loading incorporated z_{secchi} and Chl-a as explanatory variables (Spears et al., 2012; Carter and Dzialowski, 2012).

Internal loading (Spears et al., 2012), increased turbidity (Zou et al., 2020) and turnover events such as algal blooms (Wang et al., 2021) are usually associated with Peak TP concentration. Additionally, in highly eutrophic ecosystems the link between TP and algal is mutually reinforced under the internal loading perspective. This loading is more bioavailable, then more influential on algal biomass. Particularly in shallow water bodies, a continuous mixing at the sediment-water interface ensures P availability for the algal growth (Tammeorg et al., 2020). In contrast, bloom-forming cyanobacteria have a high phosphorus release potential during their decline period (Wang et al., 2021).

3.2. Phosphorus release rate and internal P load quantification

3.2.1. Net internal load and gross internal load estimation

The results of the daily gross release rates are presented in Fig. 4a while net, gross and external loads averaged over the dry period are shown in Fig. 4b. The first highlight is for the variability among the models. RR_1 and RR_2 estimates resulted in similar values in median terms, though the second one was more variable. On the contrary, RR_3 presented the lowest in-lake variability and the largest among-lakes one. This is mostly due to the reservoirs' age, that varied from 6 (R21) to 113 (R26) years. As for RR_4 estimates, although they showed higher values than those previously mentioned, the highest estimates were obtained when TP_s data was applied (RR_5).

TP_s ranged from 118.25 to 3020 mg kg^{-1} with 50th percentile of 1024 mg kg^{-1}. The highest values were observed in the older reservoirs (>900 mg kg^{-1} in reservoirs older than 58 years at the measurement date). TP_s values in other reservoirs of the Brazilian semiarid were about 600 mg kg^{-1} (Cavalcante et al., 2021) while in other regions world-wide reached 1424 mg kg^{-1} (Kim et al., 2004; Li et al., 2013; Zhang et al., 2016). As RR_5 directly incorporated these high TP_s data (Eq. (6)), high estimates were obtained accordingly. Exceptionally for R22, R23 and R25, TP_s was 2,040, 1600 and 3020 mg kg^{-1} which resulted in RR_5 estimates of 67, 86 and 127 mg m^{-2} day^{-1}, respectively (not shown in Fig. 4a). Consistently, R22 and R23 have a highly urbanized catchment and showed the highest $TP_{surface}$ values (Table 1). Similarly, for R25 a district of about 20,000 inhabitants is located near the reservoir dam with small settlements in the margins of its main tributaries. Thus, an accumulation of the intense external P pollution is pottentially occurring in the sediments of these ecosystems.

From the correlation analysis between RR_5 and the other estimates, RR_4 best performed with an r^2 of 0.36, a r_d of 0.78 and a MAPE of 39%, which were considered satisfactory indicators (Moriasi et al., 2015). The effect of the temperature, not considered in the other models, has strongly impacted RR_4 and turned Eq. (5) the more representative model for the region. RR_4 estimates ranged from 5.29 to 52.58 mg m^{-2} day^{-1} while the 50th ranged from 17.64 to 35.99 mg m^{-2} day^{-1}. In comparison with other studies, the release rates of the study sites were higher in average. However, the range observed in the searched literature varied from 1 to 77.83 mg m^{-2} day^{-1} (Arunbabu et al., 2014) with higher estimates (>50 mg m^{-2} day^{-1}) usually found in hypereutrophic ecosystems (Nurnberg, 1988). Then, RR_4 was applied along with AF to calculate the seasonal averages (Fig. 4b) considering its representativeness for the validated reservoirs.

The AF values reached 97.33 days dry $period^{-1}$ with average values ranging from 40.35 to 75.71 days dry $period^{-1}$. The lowest values were observed in the reservoirs with better water quality conditions (R3 and R13). Other studies reported values reaching 26.6 days $summer^{-1}$ (Nürnberg et al., 2013), 34.3 days Aug–Sep^{-1} and 60 days $summer^{-1}$ (Nürnberg et al., 2019, 2019b) and ~70 days $season^{-1}$ (Snortheim et al., 2017). The results suggested anoxic periods that, in some years, lasted

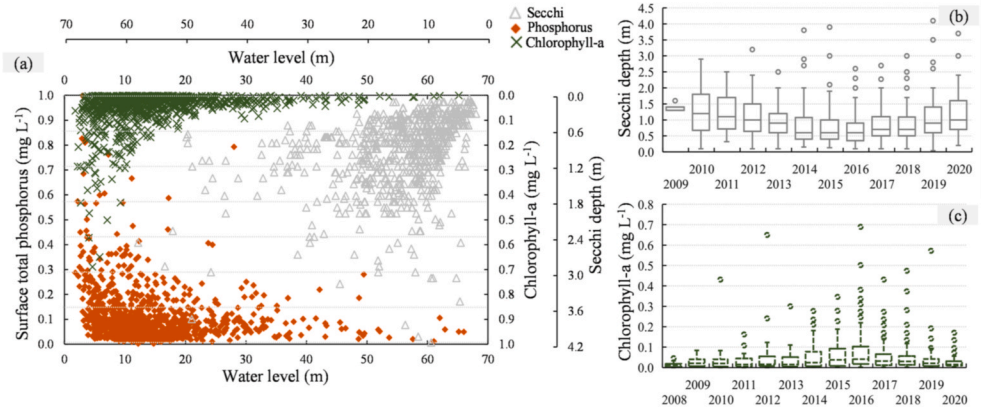

Fig. 3. (a) Water-depth related patterns of the water quality indicators Chl-a, $TP_{surface}$ and z_{secchi}* and temporal trends of (b) z_{secchi} and (c) Chl-a concentration over the study period.
* z_{secchi} data plotted in the third floating x-axis and y-axis.

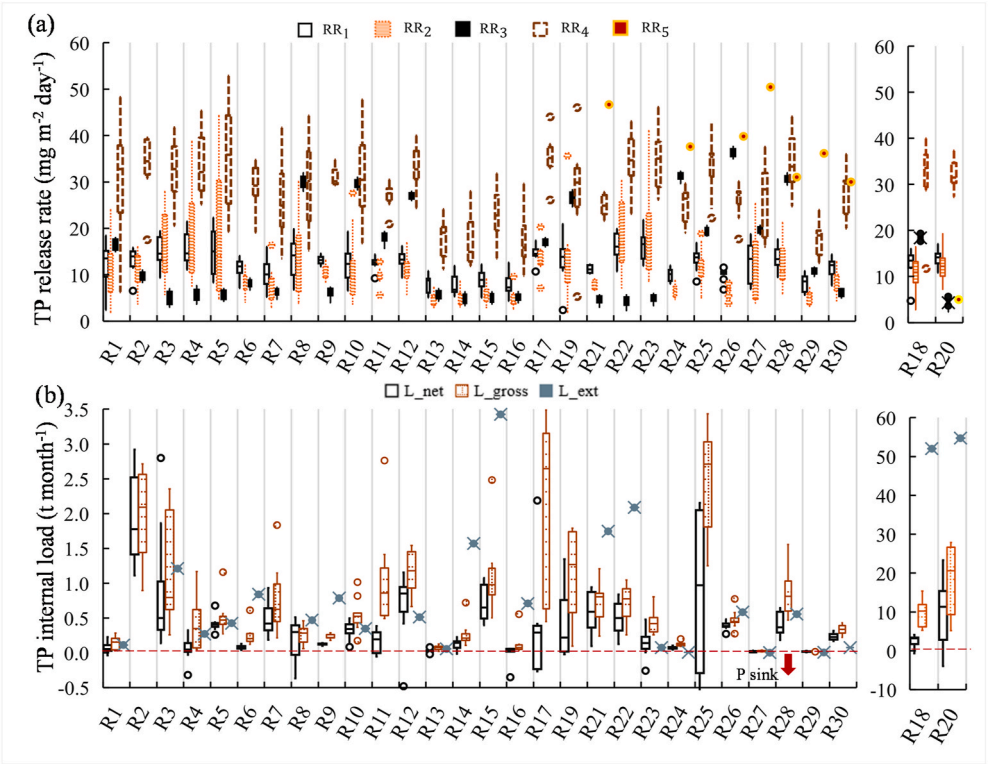

Fig. 4. (a) Daily phosphorus gross fluxes and (b) seasonal average net, gross and external TP load.
RR_1: Nurnberg (1988); RR_2: Carter and Dzialowski (2012); RR_3: Moura et al. (2020); RR_4: Cheng et al. (2020); RR_5: Chapra and Canale (1991) and Lira et al. (2020) from measured sediment data from Ceará (2021).

longer than observed in other regions. Aspects such as historical anthropogenic P supply, long periods with low DO concentration allied with lake morphometry are generally associated with hypolimnetic anoxia (Nürnberg et al., 2019). Furthermore, air temperature and wind speed are additional drivers positively correlated with AF (Nürnberg et al., 2019b). It is also noteworthy the possibility of under/-overestimated AF values. Overestimation occurs in shallow lakes since its sediment often exhibits narrow anoxic layers (Tammeorg et al., 2020), while underestimation occurs in deep lakes when the anoxic areas extend into shallow zones (Nürnberg et al., 2019b).

The average seasonal estimates (Fig. 4b) varied from 0.02 to 11.35 t month^{-1} with average of 0.26 t month^{-1}. The comparison with the external load (L_ext) showed that L_ext was over the 75th of L_net estimates in 76% of the study sites. Most catchments of the study sites are majorly rural and P external sources are the main pollution sources in the annual P budget (see Fig. S7) (Rocha and Lima Neto, 2021b). Specifically, R18 and R20 have the largest catchments (>24,000 km^2) with livestock production, subsistence farming and relevant irrigated croplands for the state (Ceará, 2021). These aspects support their high external TP production. Intensive cropland practice in a catchment favors sediment P accumulation in the waterbody in a long-term perspective (Carter and Dzialowski, 2012). Overall, 73% of the reservoirs presented the ratio between median L_net and L_ext less than 66% in accordance with was already reported by Rocha and Lima Neto (2021a), highlighting the relevance of the internal sources to the total P budget.

Unmentioned aspects so far such as sediment heterogeneity, physical characterization and size distribution may have contributed with the high estimated rates. Smaller particles have greater specific surface area for pollutant adsorption which enhances resuspension ability (Zhu and Yang, 2018). Additionally, substantial P diffusive fluxes in the warmer season may occur under oxygenated bottom water conditions from the littoral/shallow areas of the lake (Markovic et al., 2019). The littoral sediments under aerobic conditions may contribute with more than 25% of the internal phosphorus load (Kim et al., 2003; Tammeorg et al., 2017; Kowalczewska-Madura et al., 2019a). Furthermore, although P speciation data was not available, ion (Fe_s) and aluminum (Al_s) sediment concentration were measured for R21 to R30. Though more information on sediment chemical composition may be enlightening, the susceptibility of the reservoirs to metal-bound P release, specially under alkali-anoxic conditions, can be speculated (Cavalcante et al., 2021).

According to an empirical model proposed by Moura et al. (2020) for semiarid reservoirs to estimate sediment concentration of P bound to iron and aluminium (P_{FeAl}), a reservoir 42 years old (average of the study sites) should have an amount of P_{FeAl} near to 714 mg kg^{-1}. For the study sites, these two compounds presented a positive correlation with TPs, but a more significant correlation was found between the ratios Fe_s:TP_s and Al_s:TP_s with an R^2 of 0.74. Ratios of metals and P are indicative of the underlying processes controlling P release and retention (Markovic et al., 2019) and may act as operational targets on the estimation of sediment P release potential. For the study sites, the ratios Fe_s:TP_s and Al_s:TP_s varied from 4.8 to 46.5 and 2.6 to 27, respectively. Jensen et al. (1992) observed the largest difference between TP_s and TP_w in lakes when Fe:P ratios were between 10 and 15, while Kopáček et al. (2005) provided thresholds for the Al:P ratio beyond which P release may be negligible (Al:P > 25 and Al:Fe > 3). For the study sites the average ratios Al_s:TP_s and Al_s:Fe_s were 14.5 and 0.44, respectively, suggesting a high release potential.

3.2.2. *Average seasonal net internal release rates*

The estimates ranged from the most extreme values −4763.09 to 5930.63 mg m^{-2} dry period^{-1} in R19 and R5 respectively, with average of 991 mg m^{-2} dry period^{-1} (±944). Negative estimates were calculated which means that P loss processes surpassed releasing mechanisms eventually. However, positive estimates prevailed in 92.8% of the values. Although relatively high values were observed, they were

punctual estimates influenced by sensible parameters and reflected particular situations. For R19, this estimation occurred in 2009 with a decrease in TP concentration from August to November from 0.473 to 0.204 mg L^{-1}. As 2009 was the rainiest year of the study period, it is believed that the high and abrupt input of external load in this period mixed, increased the concentration during the rainy season and then promoted a slow return to a lower level in the dry period. This process implied a settling process far superior than releasing events. For R5, the load estimate resulted from a TP concentration change from 0.278 to 0.574 mg L^{-1} in August to November. These concentrations were about 9 to 19-fold higher than the limiting concentration of 0.03 mg L^{-1} established by the National Environmental Agency (Brazil, 2005). Table S1 summarizes the statistics of the estimates encompassing all study sites.

The implications associated with high internal P loading in reservoirs regard mainly the aquatic ecological functioning and the risk of eutrophication, what is especially impactful in drinking water supply reservoirs. Due to the internal P release a high trophy level tends to persist in the long-term, even minimizing the external inputs, in addition to the risk of frequent algal blooms. A direct effect is the increase in the treatment costs of the water for human consumption. From a management perspective, mitigation strategies direct on the internal load, such as artificial aeration and/or sediment dredging, are very cost demanding. In the study area, where there are about two-hundred strategic reservoirs managed by the water management company of the state, these strategies are unpractical on a large scale. Take measures upon the aquaculture practice, however, is the one viable management approach in a short-term perspective.

Apart from the extreme values already discussed, reservoir R16 presented the lowest values, followed by R13, while R8 presented the highest ones. Accordingly, R16 remained oligotrophic 45% of the study period while R13 remained mesotrophic 68%, both with low TP_w over time (Fig. 2). In addition, peak values sensitively influenced the variability on the estimates evaluated through the CV. However, disregarding these peak estimates, the obtained CV was within the ranges reported in the literature for internal load estimation (0.33–0.83) (Spears et al., 2012; Nürnberg et al., 2019; 2012, 2019; Horppila et al., 2017).

Previous studies that attempted to estimate P release rates in the warmer season have shown a range from 94 to 2117 mg m^{-2} $summer^{-1}$ (Nürnberg et al., 2012, 2013, 2019; Tammeorg et al., 2020), while long-term annual averages reached even higher values (−1694 to 10, 640 mg m^{-2} yr^{-1}) (Köhler et al., 2005; Horppila et al., 2017; Orihe et al., 2017). The higher estimates obtained in this study in comparison to other average rates reported mostly for temperate ecosystems are consistent as the amount of phosphorus released from the sediments is enhanced in warmer climate (Cheng et al., 2020). An increase in temperature by 10 °C might induce an increase in TP release by 2–7 times (Nürnberg et al., 2019). In fact, Brazilian semiarid reservoirs have water temperature (~30 °C) about 3-fold and 1.5-fold higher than temperate (~10 °C) and tropical (~20 °C) lakes, respectively. Additionally, there is the trophic status influence. As the reservoirs remained mostly eutrophic (Table 1) and with lower flows due to the drought period, higher P release rates are more likely to occur under these conditions (North et al., 2015).

3.3. The influence of trophic status and water level fluctuation on internal P load trends

Fig. 5 summarizes TSI, Chl-a and z_{secchi} for different ranges of P release in a grouped analysis of all study sites. Additionally, Fig. 5 shows the predominant trophic state over the study period for each reservoir. To improve visualization, the y-axis scale was reduced and the few values under −3000 mg L^{-1} were not shown. About 77% of the reservoirs remained eutrophic/hypereutrophic more than 50% of the time. The release rates increased across the trophic gradient being, on average, 184.86, 618.94, 752.20, and 1844.85 mg m^{-2} dry $period^{-1}$ for oligotrophic, mesotrophic, eutrophic, and hypertrophic status, respectively. The TSI is one of the main drivers of internal P loading that is hypothesized to be much higher in hypereutrophic lakes compared to lakes of lower trophic state (Carter and Dzialowski, 2012; Qin et al., 2016). This assumption was confirmed for the study sites where the differences among estimates under a hypereutrophic status and other groups were significant at a 99% level. The ratio between the release rate in a hypereutrophic and a mesotrophic environment may reach up to 6-fold (Kowalczewska-Madura et al., 2015). Additionally, P release rate increased as Chl-a increased (Fig. 5b, $p < 0.01$) and decreased as z_{secchi} increased (Fig. 5c, $p < 0.01$). This may be explained as the blue-green algae bloom and eutrophication trigger a regime shift from the clear to the turbid water and leads to the loss of submerged macrophytes which are essential for direct P uptake and increase sediment P-binding capacity. Overall, this algae contributes to increasing P release (Zhang et al., 2017).

An important consequence of the elevated productivity in eutrophic systems is anoxia (Snortheim et al., 2017). Internal loading is sometimes sufficient to maintain an eutrophic status even after external P sources reduction or elimination (Qin et al., 2016). Then, a stable mesotrophic condition is only achieved after a substantial reduction of these loadings (Lepori and Roberts, 2017) or after several times the lake hydraulic retention time on recovery (Ostrofsky and Marbach, 2019). Prolonged

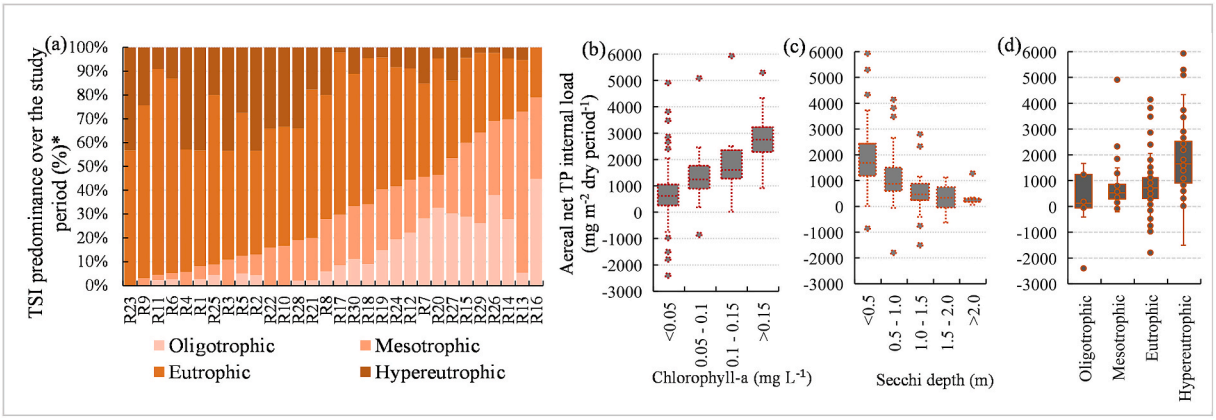

Fig. 5. (a) Distribution of the type of trophic status attributed to the reservoir by the measurement campaigns over the study period*. Trends of the seasonal net release rates with (b) Chl-a, (c) z_{secchi} and (d) trophic state.

* Calculated from the sum of each trophic classification assigned to the reservoir by measurement campaign in relation to the total of campaigns carried out in the study period.

water quality recovery after external load reduction was already verified in other semiarid ecosystems in the study region (Freire et al., 2009). Other aspects, such as the temperature gradient between water and sediment (Kowalczewska-Madura et al., 2015), catchment soil erosion and landuse (Carter and Dzialowski, 2012), high intensity of solar radiation (Santos et al., 2014), volume reduction under dry conditions (Rocha Junior et al., 2018) and aquaculture practice (Rocha Junior et al., 2018), also contribute to the worsening on the trophic state. Ultimately, the water level fluctuation (WLF) is an additional driver that can further intensify eutrophication symptoms (Cavalcante et al., 2021; Lima Neto et al., 2022).

3.4. Water level fluctuation relationship with interannual internal P load trend

The relation between lake level fluctuation as consequence of the seasonal and interannual volume reduction and the interannual variability in P estimates is shown in Fig. 6. From 2009 to 2017 the volume decreased continuously as a result of a drought event. The WLF (considering the water level difference between the two dates on which the TP measurements were performed) was on average −1.16 m, varying from −0.2 to −5.71 m annually. The sharpest WLF was observed in the largest reservoirs (R17, 20 and R25) in the driest years (2013–2016). The relative fluctuation varied from 2, mostly in 2009 when the reservoirs were full, to near 0.06 in 2015, during the lowest depths, with a steepest decrease observed from 2009 to 2013. On the opposite, a pronounced increase in the release rates was observed during the same period. From 2013 to 2016 the averages remained stable and then started a slow decrease. Analyzing the interannual variability in the release rates, significant statistical differences resulted from the paired analysis between the years 2009 and 2013–2020 ($p < 0.05$) and between the years 2012 and 2013–2016 ($p < 0.01$), when the reservoirs were gradually drying up. Similarly, significant differences ($p < 0.05$) were observed between 2015 and 2016 with the years 2019–2020, when the reservoirs were in a volume recover.

Large seasonal and annual WLF have a critical influence on the phosphorus dynamics of reservoirs in the semiarid climate zone, especially the shallower ones (Coppens et al., 2016). Unluckily, these regions are highly vulnerable to droughts which enhances WLF and volume decrease (Brasil et al., 2016). Under these conditions regime shifts or sudden transitions from one stable state to another are more likely (Huang et al., 2021) and the release capability increases with the strong disturbance intensity (Tong et al., 2017). Furthermore, in deeper lakes water level fluctuations also influence the internal nutrient mixing (Gownaris et al., 2018). Direct and inverse relationships between WLF and limnological variables such as dissolved oxygen, TP, TN, N:P ratio, total phytoplankton biomass and euphotic depth are widely known (Yang et al., 2016; Gownaris et al., 2018). To evaluate the temporal scale when considering WLF impacts is also important, as interannual and seasonal fluctuations did not influence the same ecosystem attributes.

Some researchers suggest the water level management in small and medium-sized reservoirs to reduce WLF potential negative effects on the ecosystems (Yang et al., 2016; Huang et al., 2021). However, the study sites are exposed to high evaporation rates (~2 m yr^{-1}) and recurrent drought events. These conditions turn unpractical WLF control, so the waterbodies respond freely to the environmental drivers. Furthermore, aquatic ecosystems globally are likely to become more vulnerable to extreme WLF due to the combined effects of climate change and human activity (Fu et al., 2021), and the severity of droughts may be intensified in arid environments.

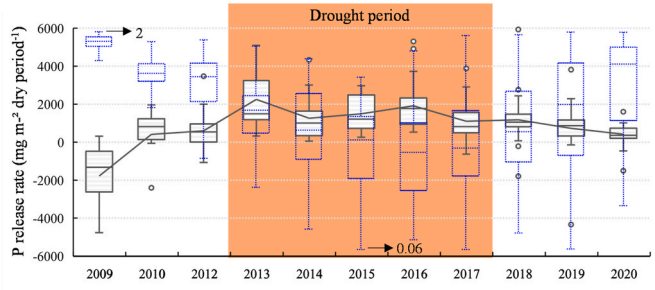

Fig. 6. TP release rate trends and WLF relative to the mean maximum depth over the study period.

3.5. Physical and environmental drivers influencing P release

Fig. 7 summarizes the grouped analysis of the climatic surrogates, their seasonality and the potential relations and impacts in the water quality parameters and in the estimated P release rate. As observed from Fig. 7b and c, the climate in the study region is markedly hot with intense insolation in the dry period in comparison to the wet one. The insolation has the sharpest variation over the months. Although there is a seasonality in the temperature, there is only a narrow variation throughout the dry period (28.2 ± 0.6 °C). To evaluate the trends in Chl-a, TP_w and P release rate depending on the range of the climatic variables, some aspects should be noticed. Firstly, for temperature and insolation, as the measurement of the water quality parameters occurred mostly in August and November and the climatic stations presented similar values for these forcings during the dry period, the average over the measurement period favored one category and the threshold limits were very close. For the wind speed, however, a wider range was evaluated.

Firstly, the wind speed was classified into three groups: below 2.5 m s^{-1} (low speed), 2.5–3.5 m s^{-1} (mild speed) and over 3.5 m s^{-1} (high speed), similar with grouping propositions adopted in other studies (Zhang et al., 2017). Wind velocity ranged from 1.3 m s^{-1} in July to 5.2 m s^{-1} in November, with an average of 3.4 m s^{-1} (±0.8). The paired analysis resulted in significant p-value ($p < 0.05$) for the three parameters evaluated. Increasing Chl-a, TP_w and P release was observed as wind speed increased. The differences were more significant ($p < 0.001$) for TP_w when comparing low speeds with high speeds. Similarly, for P release the most significant differences ($p < 0.005$) were observed between mild and high speeds.

TP_w increased from 0.05 to 0.09 mg L^{-1}, Chl-a from 0.01 to 0.03 mg L^{-1} and P release from 508.5 to 1006.1 mg m^{-2} dry $period^{-1}$ as wind changed from low to high speed. Increasing TP_w along with increasing wind speed was already found in other eutrophic reservoir in the study region (Mesquita et al., 2020). Similarly, Huang et al. (2021) studying a large Chinese shallow lake found that the TP release doubled as wind speed increased by roughly 2.2-fold. On the other hand, between mild and high speeds there was no significant differences for P release ($p = 0.32$), which suggested a stabilizing pattern of wind disturbance influencing P resuspension. Threshold wind speed that exceeds critical shear stress and trigger resuspension is still variable in literature (3–6 m s^{-1}) (Zheng et al., 2015; Jalil et al., 2019; Araújo et al., 2019; Wang et al., 2021). In this study the value of 3.5 m s^{-1} was observed as already promoting significant disturbance in lake response.

For the temperature influence, significant differences ($p < 0.005$) were observed for TP_w and Chl-a between the groups (27–27.5 °C) and (>27.5 °C) with a decrease in these parameters as temperature increased. Although there was an increase in the values when temperature changed from (<27 °C) to the other groups, as the number of observations is unequal and small for low temperature values, the statistical analysis resulted in no significant differences. Zhang et al. (2020) also found that the TP_w response to different intervals of air temperature could be and increase or decrease in concentration. As previously mentioned, the range of variation in the air temperature was very narrow (25 °C – 29 °C), with mostly high values (minimum of 25.5 °C), in comparison with the water temperature (24 °C – 32 °C). When analyzing paired data between TP_w and water temperature, a positive correlation

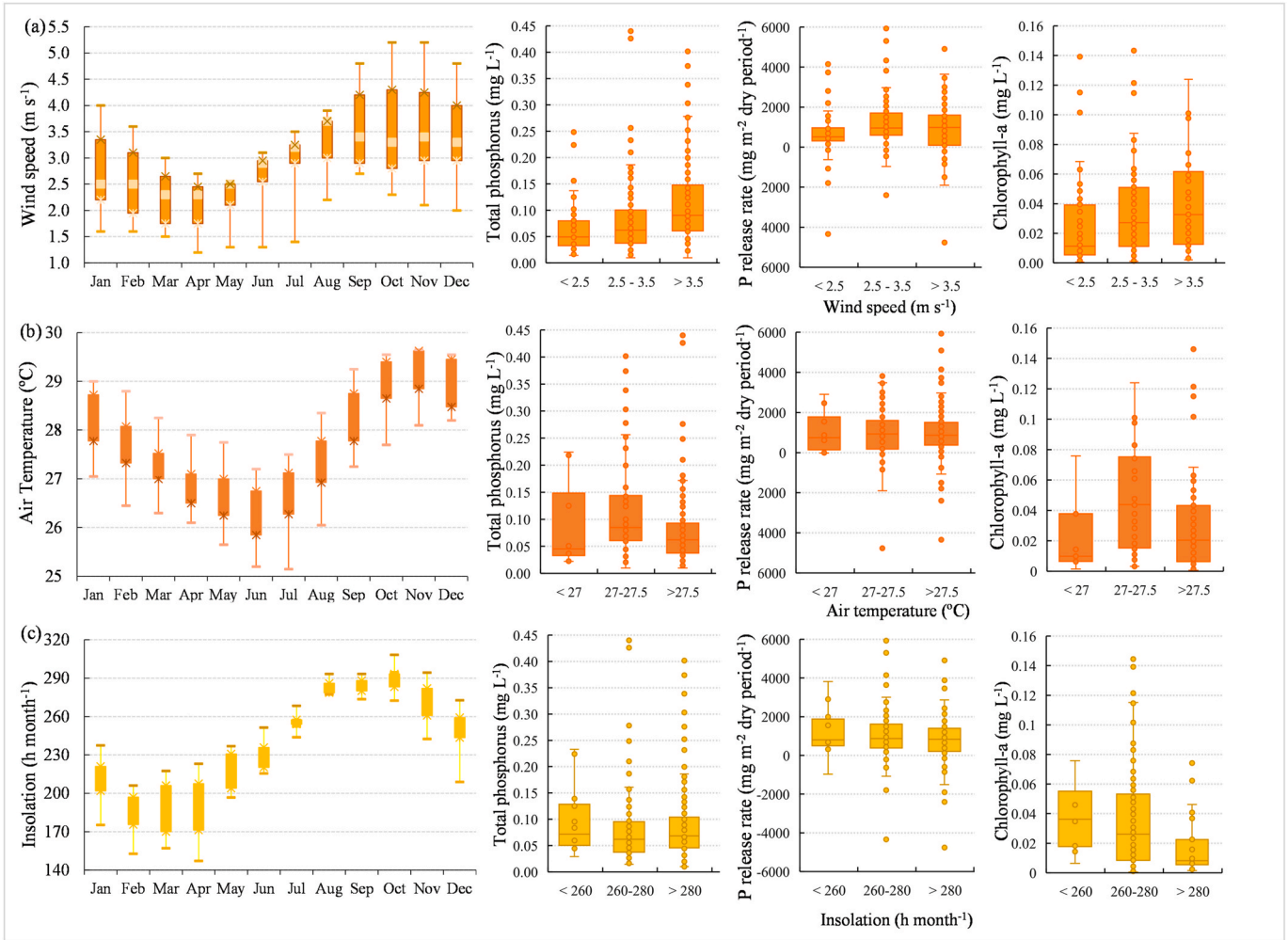

Fig. 7. Boxplot showing monthly and seasonal variation of the climatic variables wind speed, air temperature and insolation and trends of the water quality indicators and the internal P release with the categories of this climatic surrogates.

with increasing TP_w was observed. Statistically significant differences were obtained between groups (T < 25 °C) and (T > 30 °C) as expected. Note that validating water quality degradation with temperature increase usually requires final temperature significantly higher than the initial one (Zhang et al., 2016).

As for the response in P release, a slight increase in the median values was observed as temperature increased. Increasing air temperature followed by increasing water temperature partially explain the increasing trend in internal load (Nürnberg and LaZerte, 2016). Higher P release rates are expected under high temperatures (Cavalcante et al., 2021), which was actually observed in the study sites. Regarding the response of Chl-a for both temperature and insolation forcings, significant differences were observed with a decrease in concentration as these drivers increased. Studies about the phytoplankton response to light reported a growth-irradiance curve based on the continuous light exposure and a sensitive response to light fluctuation (Litchman, 2000). Depending on the species, the curve has a maximum growth rate level regardless of radiance increase, while others have a decrease pattern after a certain irradiance level. Irradiance is tolerated until a limiting, saturating and inhibiting level beyond which the species decrease in number.

3.6. Ratio between wind speed and reservoir volume as an explanatory variable for sediment P release

Proposed as an explanatory variable to the internal loading production, the ratio of wind speed to reservoir volume was correlated with the net areal TP release rates, as presented in Fig. 8. The applicability of surrogates involves a trade-off between accuracy in the representation of the target and transferability (Lindenmayer et al., 2015). Satisfactory r^2 (0.26–0.93 with median of 0.67) and r_a^2 (0.14–0.92 with median of 0.60) were obtained (Moriasi et al., 2015). The median MAPE was 36%. The few models with average performance, low r^2 and high MAPE, were influenced by peak estimates from significant TP increase (R13 in 2016 and R15 in 2014) or a sharp decrease (R12 in 2017) over the dry period for specific years. R8 (Fig. 8a) presented the best adjustment ($r^2 = 0.93$) and also the most complete dataset. Consistently, the shallowest reservoirs (R1, R4 and R27) presented the highest wind speed-reservoir volume ratios (Fig. 8e), while the largest ones (R18 and R20) presented the lowest ratios (Fig. 8c). The parameters of the equation and metrics of each fitted model are available in the supplementary material.

The models also presented a stabilizing rising pattern for P release, which was considered a consistent behavior as the releasing process do not increase indefinitely. A stabilizing limit may be achieved since nutrient release eventually reach an equilibrium state in SWI (Cyr et al., 2009). One possible explanation is that stronger winds trigger higher water current volatility and the dispersion of the pollutants from the most to least polluted zones (Zhang et al., 2017). Then, and overall increasing TP concentration is likely to occur in the reservoir. Furthermore, threshold values control the geochemical behavior of P in sediment – water system and adsorption processes prevail when P concentration surpasses this value. This way, the intensity of the release might be associated with TP_w, where higher P concentration implies less

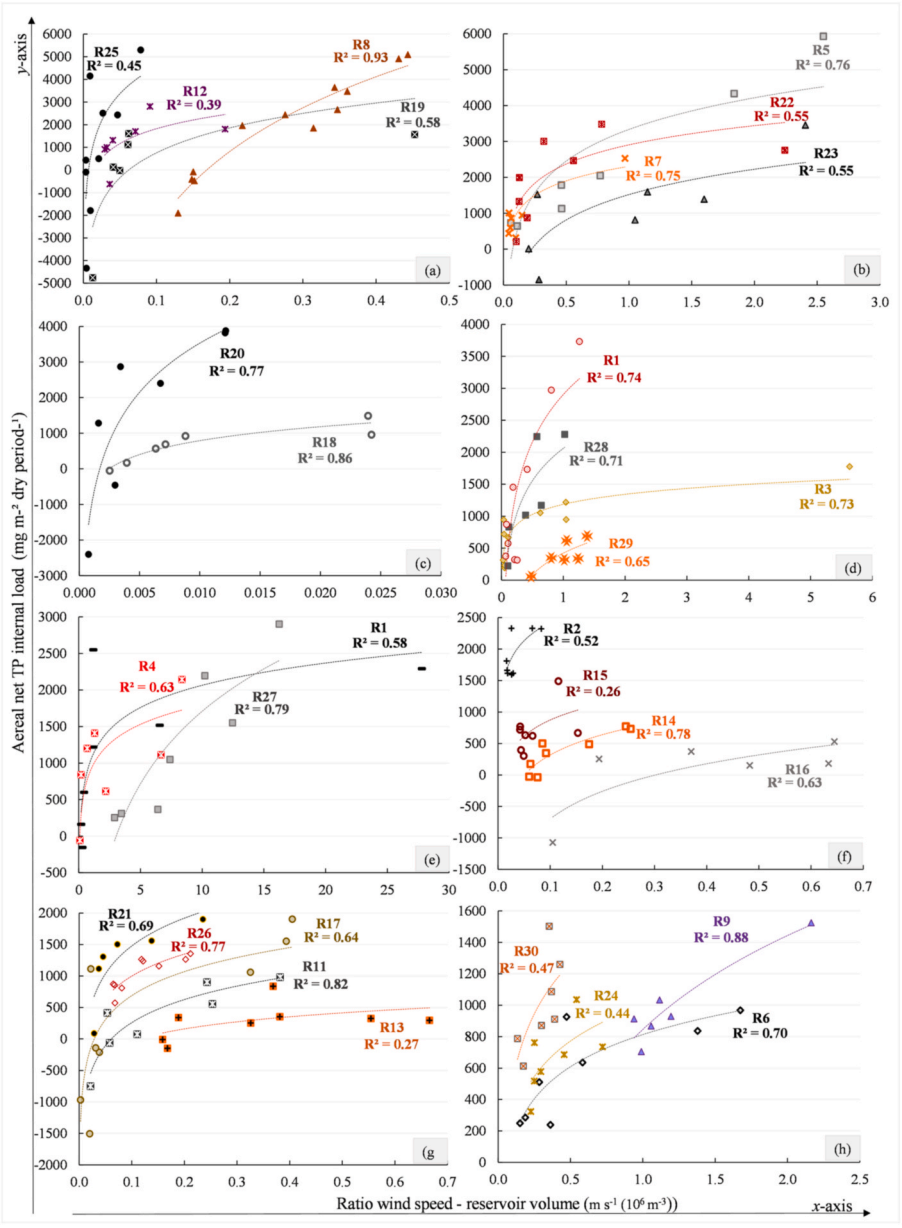

Fig. 8. Regression models developed between the ratio wind speed to reservoir volume and average seasonal TP release rate.

P release (Zhang et al., 2016).

From the obtained models and summarizing all the topics discussed in previous sections, may be inferred that the studied reservoirs accumulate several influencing aspects to the pressing internal P regeneration during the dry season such as: the instability of the water column, high water temperatures, high wind speed, high WLF, high trophic status, low DO concentrations and low water depth over the study period. Additionally, to acknowledge how these variables help the understanding of internal P loading through a study carried in a broader scale, encompassing several and different reservoirs, turns the findings and evidences more trustful. This means that each reservoir is unique but still respond similarly to others regarding the behavior of the internal P loading to a specific explanatory variable.

4. Modeling implications, uncertainty analysis and limitations

Accounting for a seasonal timescale and a long-term P budget, this work combined well stablished and novel methods of estimating internal P loading under P speciation and sediment P limited data, but sufficient water quality information. To estimate gross loads, the product of the anoxic factor with the P release rate estimated from TP_w was originally proposed by Nürnberg and LaZerte (2001) and widely applied since then (Nürnberg et al., 2019, 2012, 2013; North et al., 2015; Horppila et al., 2017; Rocha and Lima Neto, 2021a; Lima Neto et al., 2022). To obtain net loads, the classical whole-lake mass balance approach was applied (Orihe et al., 2017). This methodology is suitable to semiarid regions where strategic water supply reservoirs are threatened in the dry period by the impact of internal load to water quality deterioration. Additionally, the quantification of this important P source is favored by the intermittent regime of the rivers and a dry period of negligible inflow.

Low variability on the estimates, as already discussed through the coefficient of variation, reinforced the modeling predictive ability to estimate with acceptable accuracy seasonal loads under long term studies. As for model sensitiveness, the variability in the volume and the ratio $TP_w/TP_{w,0}$ was evaluated. The indicator $TP_w/TP_{w,0}$ was more impactful because the occurrence of considerable TP increase or decrease in a short time interval imply that extreme load input have occurred, which results in significant under/overestimation. The 75th of the ratio

$TP_w/TP_{w,0}$ was 1.48 with average of 1.25, which is slightly lower than the suggested threshold of 1.5 (Rocha and Lima Neto, 2021a). As for the volume impact, its large interannual variability is typical of semiarid regions and the response in the internal load estimates is supported by the associated physical and biogeochemical processes.

Limitations on modelling may occur due to potential underestimation or overestimation of the net release rates (Tammeorg et al., 2020) influenced by factors such as: (i) use of average concentrations (Nikolai and Dzialowski, 2014), (ii) spatial variability due to sediment heterogeneity, (iii) quantification of anoxia extent by the anoxic factor and (iv) under representation of extreme values as samples of deeper depths were not always available. However, despite eventual inaccuracies intrinsic of the modeling process, the estimates seem reasonable since: (i) they are corroborated by several independent approaches, (ii) the mass balance approach is enhanced when calculating multiyear averages and (iii) they were significant when compared to external inputs. Furthermore, the reservoirs accumulated several influencing aspects to the pressing internal P estimated, as already discussed in the previous section.

5. Conclusions

This study assessed the long-term internal P loading contribution in thirty strategic water supplies reservoirs located in the Brazilian semiarid. Net and gross release estimates were obtained by seasonal P budget and regression approaches accounting for the components water column and sediment TP concentration, anoxic duration, water temperature, fish contribution and reservoir age. Further analyses statistically connected the estimates with in-lake water quality indicators, physical surrogates, and environmental drivers. Finally, a new indicator was proposed along with predictive regression models to enable P release estimation from easily available data.

The average seasonal net estimates were 991 mg m^{-2} dry $period^{-1}$ (±944), while average gross estimates varied from 17.64 mg m^{-2} day^{-1} to 35.99 mg m^{-2} day^{-1}. The rates were slightly higher than reported for temperate ecosystems, which may be attributed to the enriched sediments allied with warmer water temperature and prolonged anoxic periods. Furthermore, the average P release rates significantly increased across the trophic gradient ($p < 0.05$), about 10-fold higher under hypertrophic status than in oligotrophic one. The results also indicated that the highest releases occurred in the driest years with the reservoirs in their lowest volumes.

Regarding the predictive models for P release, the coupling of the wind speed with the mean reservoir volume proved to be a strong surrogate to estimate sediment P release (r^2: 0.26–0.93). The behavior of the adjusted models was physically consistent. A stabilizing pattern was achieved since there is a threshold P concentration in SWI that restricts unlimited P release. This surrogate also balanced accuracy and transferability, in order to be replicable to other regions. Despite modelling uncertainties, the obtained results are supported since the study sites accumulated several influencing aspects for the internal P production during the dry season. Additionally, independent methodologies supported each other. Especially in dryland regions where water supply reservoirs are under critical water quality and environmental conditions, the finding of this study may help to support phosphorus pollution management strategies.

Credit author statement

Maria de Jesus Delmiro Rocha: Conceptualization; Data curation; Formal analysis; Investigation; Methodology; Validation; Writing – original draft. **Iran Eduardo Lima Neto**: Conceptualization; Formal analysis; Funding acquisition; Project administration; Supervision; Writing – review & editing.

Declaration of competing interest

The authors declare that they have no known competing financial interests or personal relationships that could have appeared to influence the work reported in this paper.

Acknowledgements

The present study was supported through the Ceará State Research Foundation - FUNCAP [Research Grant PNE-0112-00042.01.00/16] and the Coordination for the Improvement of Higher Education Personnel - CAPES [Research Grant PROEX 04/2021]. The authors would like to thank the Water Resources Management Company of the State of Ceará (COGERH) for providing the data necessary for the analyses.

Appendix A. Supplementary data

Supplementary data to this article can be found online at https://doi.org/10.1016/j.jenvman.2022.114983.

References

Andrade, E.M., Ferreira, K.C.D., Lopes, F.B., Araújo, I.C. da S., da Silva, A.G.R., 2020. Balance of nitrogen and phosphorus in a reservoir in the tropical semiarid region: balanço de nitrogênio e fósforo em um reservatório na região semi-árida tropical. Rev. Cienc. Agron. 51, 1–10. https://doi.org/10.5935/1806-6690.20200020.

Araújo, G.M., Lima Neto, I.E., Becker, H., 2019. Phosphorus dynamics in a highly polluted urban drainage channelshallow reservoir system in the Brazilian semiarid. An. Acad. Bras. Cienc. 91 https://doi.org/10.1590/0001-3765201920180441.

Arunbabu, E., Ravichandran, S., Sreeja, P., 2014. Sedimentation and internal phosphorus loads in Krishnagiri Reservoir, India. Lakes Reservoirs Res. Manag. 19, 161–173. https://doi.org/10.1111/lre.12069.

Barbosa, J. do S.B., Bellotto, V.R., da Silva, D.B., Lima, T.B., 2019. Nitrogen and Phosphorus Budget for a Deep Tropical Reservoir of the Brazilian Savannah, vol. 11. Water, Switzerland. https://doi.org/10.3390/w11061205.

Brasil, J., Attayde, J.L., Vasconcelos, F.R., Dantas, D.D.F., Huszar, V.L.M., 2016. Drought-induced water-level reduction favors cyanobacteria blooms in tropical shallow lakes. Hydrobiologia 770, 145–164. https://doi.org/10.1007/s10750-015-2578-5.

Brazil, 2005. Ministério do Meio Ambiente: Conselho Nacional de Meio Ambiente. CONAMA. Resolução CONAMA nº 357, de 17 de março de 2005. Disponível em: http://www.mma.gov.br. Acesso em: 04 mar 2021.

Brazil, 2021. Instituto Nacional de Meteorologia. Normais climatológicas. Disponível em: https://portal.inmet.gov.br/normais>. Acesso em. (Accessed 17 January 2021).

Carneiro, F.M., Nabout, J.C., Vieira, L.C.G., Roland, F., Bini, L.M., 2014. Determinants of chlorophyll-a concentration in tropical reservoirs. Hydrobiologia 740, 89–99. https://doi.org/10.1007/s10750-014-1940-3.

Carter, L.D., Dzialowski, A.R., 2012. Predicting sediment phosphorus release rates using landuse and water-quality data. Freshw. Sci. 31, 1214–1222. https://doi.org/10.1899/11-177.1.

Cavalcante, H., Araújo, F., Noyma, N.P., Becker, V., 2018. Phosphorus fractionation in sediments of tropical semiarid reservoirs. Sci. Total Environ. 619–620, 1022–1029. https://doi.org/10.1016/j.scitotenv.2017.11.204.

Cavalcante, H., Araújo, F., Becker, V., de Lucena Barbosa, J.E., 2021. Internal phoshorus loading potential of a semiarid reservoir: an experimental study. Acta Limnol. Bras. 33, 1–13. https://doi.org/10.1590/s2179-975x10220.

Ceará, 2021. Companhia de Gestão dos Recursos Hídricos: Monitoramento Quantitativo e Qualitativo dos Recursos Hídricos. Disponível em: <http://www.hidro.ce.gov.br>. Acesso em: 25 abr. 2021.

Ceará. Bureau, 2018. Of Water Resources of the Government of the State of Ceará. Plan of Strategic Actions in Water Resources of the State of Ceará. Available in: https://www.srh.ce.gov.br/wp-content/uploads/sites/90/2018/07/PLANO-DE-ACOES-ESTRATEGICAS-DE-RECURSOS-HIDRICOS-CE_2018.pdf.

Chapra, S.C., Canale, R.P., 1991. Long-term phenomenological model of phosphorus and oxygen for stratified lakes. Water Res. 25, 707–715. https://doi.org/10.1016/0043-1354(91)90046-S.

Chaves, F.Í.B., Lima, P. de F., Leitão, R.C., Paulino, W.D., Santaella, S.T., 2013. Influência da chuva no estado trófico de um reservatório do semiárido Brasileiro. Acta Sci. Biol Sci. 35, 505–511. https://doi.org/10.4025/actascibiolsci.v35i4.18261.

Cheng, X., Huang, Y., Li, R., Pu, X., Huang, W., Yuan, X., 2020. Impacts of water temperature on phosphorus release of sediments under flowing overlying water. J. Contam. Hydrol. 235, 103717. https://doi.org/10.1016/j.jconhyd.2020.103717.

Cleophas, T.J., Zwinderman, A.H., 2016. Non-parametric tests for three or more samples (friedman and kruskal-wallis). In: Clinical Data Analysis on a Pocket Calculator. Springer, Cham. https://doi.org/10.1007/978-3-319-27104-0_34.

Coppens, J., Özen, A., Tavşanoğlu, T.N., Erdoğan, Ş., Levi, E.E., Yozgatligil, C., Jeppesen, E., Beklioğlu, M., 2016. Impact of alternating wet and dry periods on long-term seasonal phosphorus and nitrogen budgets of two shallow Mediterranean lakes. Sci. Total Environ. 563–564, 456–467. https://doi.org/10.1016/j.scitotenv.2016.04.028.

Costa, R.L., Macedo de Mello Baptista, G., Gomes, H.B., Daniel dos Santos Silva, F., Lins da Rocha Júnior, R., de Araújo Salvador, M., Herdies, D.L., 2020. Analysis of climate extremes indices over northeast Brazil from 1961 to 2014. Weather Clim. Extrem. 28 https://doi.org/10.1016/j.wace.2020.100254.

Cyr, H., McCabe, S.K., Nürnberg, G.K., 2009. Phosphorus sorption experiments and the potential for internal phosphorus loading in littoral areas of a stratified lake. Water Res. 43, 1654–1666. https://doi.org/10.1016/j.watres.2008.12.050.

Dantas, E.W., Moura, A.N., Bittencourt, M.C.O., 2011. Cyanobacterial blooms in stratified and destratified eutrophic reservoirs in semi-arid region of Brazil. An. Acad. Bras. Cienc. 83, 1327–1338.

Ding, S., Chen, M., Gong, M., Fan, X., Qin, B., Xu, H., Gao, S.S., Jin, Z., Tsang, D.C.W., Zhang, C., 2018. Internal phosphorus loading from sediments causes seasonal nitrogen limitation for harmful algal blooms. Sci. Total Environ. 625, 872–884. https://doi.org/10.1016/j.scitotenv.2017.12.348.

Freire, R.H.F., Calijuri, M.C., Santaella, S.T., 2009. Longitudinal patterns and variations in water quality in a reservoir in the semiarid region of NE Brazil: responses to hydrological and climatic changes. Acta Limnol. Bras. 21, 251–262.

Fu, C., Wu, Huawu, Zhu, Z., Song, C., Xue, B., Wu, Haohao, Ji, Z., Dong, L., 2021. Exploring the potential factors on the striking water level variation of the two largest semi-arid-region lakes in northeastern Asia. Catena 198, 105037. https://doi.org/10.1016/j.catena.2020.105037.

Fukushima, T., Matsushita, B., Subehi, L., Setiawan, F., Wibowo, H., 2017. Will hypolimnetic waters become anoxic in all deep tropical lakes? Sci. Rep. 7, 1–8. https://doi.org/10.1038/srep45320.

Gownaris, N.J., Rountos, K.J., Kaufman, L., Kolding, J., Lwiza, K.M.M., Pikitch, E.K., 2018. Water level fluctuations and the ecosystem functioning of lakes. J. Great Lake. Res. 44, 1154–1163. https://doi.org/10.1016/j.jglr.2018.08.005.

Gurgel-Lourenço, R.C., Rodrigues-Filho, C.A. de S., Angelini, R., Garcez, D.S., Sánchez-Botero, J.I., 2015. On the relation amongst limnological factors and fish abundance in reservoirs at semiarid region. Acta Limnol. Bras. 27, 24–38. https://doi.org/10.1590/s2179-975x2414.

Håkanson, L., 2005. The importance of lake morphometry and catchment characteristics in limnology - ranking based on statistical analyses. Hydrobiologia 541, 117–137. https://doi.org/10.1007/s10750-004-5032-7.

Horppila, J., Holmroos, H., Niemistö, J., Massa, I., Nygrén, N., Schönach, P., Tapio, P., Tammeorg, O., 2017. Variations of internal phosphorus loading and water quality in a hypertrophic lake during 40 years of different management efforts. Ecol. Eng. 103, 264–274. https://doi.org/10.1016/j.ecoleng.2017.04.018.

Huang, J., Xu, Q., Wang, X., Ji, H., Quigley, E.J., Sharbatmaleki, M., Li, S., Xi, B., Sun, B., Li, C., 2021. Effects of hydrological and climatic variables on cyanobacterial blooms in four large shallow lakes fed by the Yangtze River. Environ. Sci. Ecotechnology 5, 100069. https://doi.org/10.1016/j.ese.2020.100069.

Hunter, M., Westgate, M., Barton, P., Calhoun, A., Pierson, J., Tulloch, A., Beger, M., Branquinho, C., Caro, T., Gross, J., Heino, J., Lane, P., Longo, C., Martin, K., McDowell, W.H., Mellin, C., Salo, H., Lindenmayer, D., 2016. Two roles for ecological surrogacy: indicator surrogates and management surrogates. Ecol. Indicat. 63, 121–125. https://doi.org/10.1016/j.ecolind.2015.11.049.

Jalil, A., Li, Y., Zhang, K., Gao, X., Wang, W., Khan, H.O.S., Pan, B., Ali, S., Acharya, K., 2019. Wind-induced hydrodynamic changes impact on sediment resuspension for large, shallow Lake Taihu, China. Int. J. Sediment Res. 34, 205–215. https://doi.org/10.1016/j.ijsrc.2018.11.003.

Jensen, H.S., Kristensen, P., Jeppesen, E., Skytthe, A., 1992. Iron:phosphorus ratio in surface sediment as an indicator of phosphate release from aerobic sediments in shallow lakes. Hydrobiologia 235–236, 731–743. https://doi.org/10.1007/BF00026261.

Jepson, W., Tomaz, P., Santos, J.O., Baek, J., 2021. A comparative analysis of urban and rural household water insecurity experiences during the 2011–17 drought in Ceará, Brazil. Water Int. 46, 697–722. https://doi.org/10.1080/02508060.2021.1944543.

Johansson, T., Nordvarg, L., 2002. Empirical mass balance models calibrated for freshwater fish farm emissions. Aquaculture 212, 191–211. https://doi.org/10.1016/S0044-8486(02)00013-3.

Katsev, S., 2017. When large lakes respond fast: a parsimonious model for phosphorus dynamics. J. Great Lake. Res. 43, 199–204. https://doi.org/10.1016/j.jglr.2016.10.012.

Katsev, S., Tsandev, I., L'Heureux, I., Rancourt, D.G., 2006. Factors controlling long-term phosphorus efflux from lake sediments: exploratory reactive-transport modeling. Chem. Geol. 234, 127–147. https://doi.org/10.1016/j.chemgeo.2006.05.001.

Kelly, L.A., 1993. Release rates and biological availability of phosphorus released from sediments receiving aquaculture wastes. Hydrobiologia 253, 367–372. https://doi.org/10.1007/BF00050762.

Kiani, M., Tammeorg, P., Niemistö, J., Simojoki, A., Tammeorg, O., 2020. Internal phosphorus loading in a small shallow Lake: response after sediment removal. Sci. Total Environ. 725, 138279. https://doi.org/10.1016/j.scitotenv.2020.138279.

Kim, L.H., Choi, E., Stenstrom, M.K., 2003. Sediment characteristics, phosphorus types and phosphorus release rates between river and lake sediments. Chemosphere 50, 53–61. https://doi.org/10.1016/S0045-6535(02)00310-7.

Kim, L.H., Choi, E., Gil, K.I., Stenstrom, M.K., 2004. Phosphorus release rates from sediments and pollutant characteristics in Han River, Seoul, Korea. Sci. Total Environ. 321, 115–125. https://doi.org/10.1016/j.scitotenv.2003.08.018.

Klippel, G., Macêdo, R.L., Branco, C.W.C., 2020. Comparison of different trophic state indices applied to tropical reservoirs. Lakes & Reservoirs: Science, Policy and Management for Sustainable Use 25 (2), 214–229. https://doi.org/10.1111/lre.12320.

Köhler, J., Hilt, S., Adrian, R., Nicklisch, A., Kozerski, H.P., Walz, N., 2005. Long-term response of a shallow, moderately flushed lake to reduced external phosphorus and nitrogen loading. Freshw. Biol. 50, 1639–1650. https://doi.org/10.1111/j.1365-2427.2005.01430.x.

Kolding, J., van Zwieten, P.A.M., 2012. Relative lake level fluctuations and their influence on productivity and resilience in tropical lakes and reservoirs. Fish. Res. 115– 116, 99–109. https://doi.org/10.1016/j.fishres.2011.11.008.

Kopáček, J., Borovec, J., Hejzlar, J., Ulrich, K.U., Norton, S.A., Amirbahman, A., 2005. Aluminum control of phosphorus sorption by lake sediments. Environ. Sci. Technol. 39, 8784–8789. https://doi.org/10.1021/es050916b.

Kowalczewska-Madura, K., Gołdyn, R., Dera, M., 2015. Spatial and seasonal changes of phosphorus internal loading in two lakes with different trophy. Ecol. Eng. 74, 187–195. https://doi.org/10.1016/j.ecoleng.2014.10.033.

Kowalczewska-Madura, K., Dondajewska, R., Gołdyn, R., Rosińska, J., Podsiadłowski, S., 2019a. Internal phosphorus loading as the response to complete and then limited sustainable restoration of a shallow lake. Ann. Limnol. 55 https://doi.org/10.1051/limn/2019003.

Kowalczewska-Madura, K., Gołdyn, R., Bogucka, J., Strzelczyk, K., 2019b. Impact of environmental variables on spatial and seasonal internal phosphorus loading in a mesoeutrophic lake. Int. J. Sediment Res. 34, 14–26. https://doi.org/10.1016/j.ijsrc.2018.08.008.

Lacerda, L.D., Santos, J.A., Marins, R.V., Da Silva, F.A.T.F., 2018. Limnology of the largest multi-use artificial reservoir in NE Brazil: the castanhão reservoir, Ceará state. An. Acad. Bras. Cienc. 90, 2073–2096. https://doi.org/10.1590/0001-3765201820180085.

Lemos, W.E.D., 2015. Seasonal Climate Forecast of the Reservoir Thermal and Hydrodynamic Regime. Thesis (Doctorate) - Civil Engineering Course. Universidade Federal do Ceará, Fortaleza, p. 166, 2015 (in Portuguese).

Lepori, F., Roberts, J.J., 2017. Effects of internal phosphorus loadings and food-web structure on the recovery of a deep lake from eutrophication. J. Great Lake. Res. 43, 255–264. https://doi.org/10.1016/j.jglr.2017.01.008.

Li, H., Shi, A., Li, M., Zhang, X., 2013. Effect of pH, temperature, dissolved oxygen, and flow rate of overlying water on heavy metals release from storm sewer sediments. J. Chem. https://doi.org/10.1155/2013/434012, 2013.

Lima, B.P., 2016. Framing of Waterbodies in the Brazilian Northeast as an Instrument for Environmental Management and Sustainability: the Case of the Acarape Do Meio Watershed in Ceará, 271 f. Thesis (Doctorate). Agricultural Engineering Course. Department of Agricultural Engineering, Federal University of Ceará, Fortaleza.

Lima Neto, I.E., Wiegand, M.C., Araújo, J.C., 2011. Sediment redistribution due to a dense reservoir network in a large semi-arid Brazilian basin. Hydrol. Sci. J. 56, 319–333. https://doi.org/10.1080/02626667.2011.553616.

Lima Neto, I.E., 2019. Impact of artificial destratification on water availability of reservoirs in the Brazilian semiarid. Anais da Academia Brasileira de Ciências 91 (3). https://doi.org/10.1590/0001-3765201920171022.

Lima Neto, I.E., Medeiros, P.H.A., Costa, A.C., Wiegand, M.C., Barros, A.R.M., Barros, M.U.G., 2022. Assessment of phosphorus loading dynamics in a tropical reservoir with high seasonal water level changes. Sci. Total Environ. 815, 152–162. https://doi.org/10.1016/j.scitotenv.2021.152875.

Lindenmayer, D., Pierson, J., Barton, P., Beger, M., Branquinho, C., Calhoun, A., Caro, T., Greig, H., Gross, J., Heino, J., Hunter, M., Lane, P., Longo, C., Martin, K., McDowell, W.H., Mellin, C., Salo, H., Tulloch, A., Westgate, M., 2015. A new framework for selecting environmental surrogates. Sci. Total Environ. 538, 1029–1038. https://doi.org/10.1016/j.scitotenv.2015.08.056.

Lira, C.C.S., Medeiros, P.H.A., Neto, I.E.L., 2020. Modelling the impact of sediment management on the trophic state of a tropical reservoir with high water storage variations. An. Acad. Bras. Cienc. 92, 1–18. https://doi.org/10.1590/0001-3765202020181169.

Litchman, E., 2000. Growth rates of phytoplankton under fluctuating light. Freshw. Biol. 44, 223–235. https://doi.org/10.1046/j.1365-2427.2000.00559.x.

Liu, Q., Ding, S., Chen, X., Sun, Q., Chen, M., Zhang, C., 2018. Effects of temperature on phosphorus mobilization in sediments in microcosm experiment and in the field. Appl. Geochem. 88, 158–166. https://doi.org/10.1016/j.apgeochem.2017.07.018.

Lopes, F.B., de Andrade, E.M., Meireles, A.C.M., Becker, H., Batista, A.A., 2014. Assessment of the water quality in a large reservoir in semiarid region of Brazil. Rev. Bras. Eng. Agrícola Ambient. 18, 437–445. https://doi.org/10.1590/S1415-43662014000400012.

Markovic, S., Liang, A., Watson, S.B., Guo, J., Mugalingam, S., Arhonditsis, G., Morley, A., Dittrich, M., 2019. Biogeochemical mechanisms controlling phosphorus diagenesis and internal loading in a remediated hard water eutrophic embayment. Chem. Geol. 514, 122–137. https://doi.org/10.1016/j.chemgeo.2019.03.031.

Meireles, A.C.M., Frischkorn, H., Andrade, E.M., 2007. Seasonality of water quality in the Edson Queiroz reservoir, Acaraú basin, in the semi-arid region of Ceará. Rev. Cienc. Agron. 38 (1), 25–31 (in Portuguese).

Mesquita, J.B.F., Lima Neto, I.E., Raabe, A., Araújo, J.C., 2020. The influence of hydroclimatic conditions and water quality on evaporation rates of a tropical lake. J. Hydrol. 590, 125456. https://doi.org/10.1016/j.jhydrol.2020.125456.

Molisani, M.M., do Monte, T.M., Vasconcellos, G.H., de Souza Barroso, H., Moreira, M.O. P., Becker, H., de Rezende, C.E., Franco, M.A.L., de Farias, E.G.G., de Camargo, P.B., 2015. Relative effects of nutrient emission from intensive cage aquaculture on the semiarid reservoir water quality. Environ. Monit. Assess. 187 https://doi.org/10.1007/s10661-015-4925-4.

Moriasi, D.N., Gitau, M.W., Pai, N., Daggupati, P., 2015. Hydrologic and water quality models: performance measures and evaluation criteria. Transactions of The Asabe 58, 1763–1785. https://doi.org/10.13031/trans.58.10715.

Moura, Diana S., Lima Neto, I.E., Clemente, A., Oliveira, S., Pestana, C.J., Aparecida de Melo, M., Capelo-Neto, J., 2020. Modeling phosphorus exchange between bottom sediment and water in tropical semiarid reservoirs. Chemosphere 246. https://doi.org/10.1016/j.chemosphere.2019.125686.

Moura, Diana Souza, De Almeida, A.S.O., Pestana, C.J., Girão, L.G., Capelo-Neto, J., 2020b. Internal loading potential of phosphorus in reservoirs along a semiarid watershed. Rev. Bras. Recur. Hidricos 25, 1–11. https://doi.org/10.1590/2318-0331.252020180023.

Nicholls, K.H., 1999. Effects of temperature and other factors on summer phosphorus in the inner Bay of Quinte, Lake Ontario: implications for climate warming. J. Great Lake. Res. 25, 250–262. https://doi.org/10.1016/S0380-1330(99)70734-3.

Nikolai, S.J., Dzialowski, A.R., 2014. Effects of internal phosphorus loading on nutrient limitation in a eutrophic reservoir. Limnologica 49, 33–41. https://doi.org/10.1016/j.limno.2014.08.005.

Noori, R., Berndtsson, R., Adamowski, J.F., Abyaneh, M.R., 2018. Temporal and depth variation of water quality due to thermal stratification in Karkheh Reservoir, Iran. J. Hydrol.: Reg. Stud. 19, 279–286. https://doi.org/10.1016/j.ejrh.2018.10.003.

Noori, R., Ansari, E., Jeong, Y., Aradpour, S., Maghrebi, M., Hosseinzadeh, M., Bateni, Sayed M., 2021a. Hyper-nutrient enrichment status in the sabalan lake, Iran. Water 13, 2874. https://doi.org/10.3390/w13202874, 1.

Noori, R., Ansari, E., Bhattarai, R., Tang, Q., Aradpour, S., Maghrebi, M., Haghighi, A.T., Bengtsson, L., Kløve, B., 2021b. Complex dynamics of water quality mixing in a warm mono-mictic reservoir. Sci. Total Environ. 777 https://doi.org/10.1016/j.scitotenv.2021.146097.

North, R.L., Johansson, J., Vandergucht, D.M., Doig, L.E., Liber, K., Lindenschmidt, K.E., Baulch, H., Hudson, J.J., 2015. Evidence for internal phosphorus loading in a large prairie reservoir (Lake Diefenbaker, Saskatchewan). J. Great Lake. Res. 41, 91–99. https://doi.org/10.1016/j.jglr.2015.07.003.

Nurnberg, G.K., 1988. Prediction ease rates from in anoxic lake. Can. J. Fish. Aquat. Sci. 45, 453–462.

Nürnberg, G.K., 1995. Quantifying anoxia in lakes. Limnol. Oceanogr. 40, 1100–1111. https://doi.org/10.4319/lo.1995.40.6.1100.

Nürnberg, G.K., 2005. Quantification of internal phosphorus loading in polymictic lakes. SIL Proceedings 29, 623–626. https://doi.org/10.1080/03680770.2005.11902753, 1922-2010.

Nurnberg, G.K., 2009. Assessing internal phosphorus load - Problems to be solved. Lake Reservoir Manag. 25, 419–432. https://doi.org/10.1080/00357520903458848.

Nürnberg, G.K., 2019. Quantification of anoxia and hypoxia in water bodies. Encycl. Water 1–9. https://doi.org/10.1002/9781119300762.wsts0081.

Nürnberg, G.K., LaZerte, 2001. Managing Lakes and Reservoirs (Chapter 1): Predicting lake water quality.

Nürnberg, G.K., LaZerte, B.D., 2016. More than 20 years of estimated internal phosphorus loading in polymictic, eutrophic Lake Winnipeg, Manitoba. J. Great Lake. Res. 42, 18–27. https://doi.org/10.1016/j.jglr.2015.11.003.

Nurnberg, G.K., Shaw, M., Dillon, P.J., McQueen, D.J., 1986. Internal phosphorus load in an oligotrophic Precambrian Shield Lake with an anoxic hypolimnion. Can. J. Fish. Aquat. Sci. 43, 574–580. https://doi.org/10.1139/f86-068.

Nürnberg, G.K., Tarvainen, M., Ventelä, A.M., Sarvala, J., 2012. Internal phosphorus load estimation during biomanipulation in a large polymictic and mesotrophic lake. Inl. Waters 2, 147–162. .org/10.5268/IW-2.3.469.

Nürnberg, G.K., LaZerte, B.D., Loh, P.S., Molot, L.A., 2013. Quantification of internal phosphorus load in large, partially polymictic and mesotrophic Lake Simcoe, Ontario. J. Great Lake. Res. 39, 271–279. https://doi.org/10.1016/j.jglr.2013.03.017.

Nürnberg, G.K., Howell, T., Palmer, M., 2019. Long-term impact of Central Basin hypoxia and internal phosphorus loading on north shore water quality in Lake Erie. Inl. Waters 9, 362–373. https://doi.org/10.1080/20442041.2019.1568072.

Orihe, D.M., Baulch, H.M., Casson, N.J., North, R.L., Parsons, C.T., Seckar, D.C.M., Venkiteswaran, J.J., 2017. Internal phosphorus loading in canadian fresh waters: a critical review and data analysis. Can. J. Fish. Aquat. Sci. 74, 2005–2029. https://doi.org/10.1139/cjfas-2016-0500.

Ostrofsky, M.L., Marbach, R.M., 2019. Predicting internal phosphorus loading in stratified lakes. Aquat. Sci. 81, 1–9. https://doi.org/10.1007/s00027-018-0618-8.

Qin, L., Zeng, Q., Zhang, W., Li, X., Steinman, A.D., Du, X., 2016. Estimating internal P loading in a deep water reservoir of northern China using three different methods. Environ. Sci. Pollut. Res. 23, 18512–18523. https://doi.org/10.1007/s11356-016-7035-0.

Rattan, K.J., Corriveau, J.C., Brua, R.B., Culp, J.M., Yates, A.G., Chambers, P.A., 2017. Quantifying seasonal variation in total phosphorus and nitrogen from prairie streams in the Red River Basin, Manitoba Canada. Sci. Total Environ. 575, 649–659. https://doi.org/10.1016/j.scitotenv.2016.09.073.

Rocha, M.J.D., Lima Neto, I.E., 2021a. Phosphorus mass balance and input load estimation from the wet and dry periods in tropical semiarid reservoirs. Environ. Sci. Pollut. Res. https://doi.org/10.1007/s11356-021-16251-w.

Rocha, M.J.D., Lima Neto, I.E., 2021b. Modeling flow-related phosphorus inputs to tropical semiarid reservoirs. J. Environ. Manag. 295, 113123. https://doi.org/10.1016/j.jenvman.2021.113123.

Rocha Junior, C.A.N. da, Costa, M.R.A. da, Menezes, R.F., Attayde, J.L., Becker, V., 2018. Water volume reduction increases eutrophication risk in tropical semi-arid reservoirs. Acta Limnol. Bras. 30 https://doi.org/10.1590/s2179-975x2117.

Santos, J.C.N., de Andrade, E.M., de Araújo Neto, J.R., Meireles, A.C.M., de Queiroz Palácio, H.A., 2014. Land use and trophic state dynamics in a tropical semi-arid reservoir. Rev. Cienc. Agron. 45, 35–44. https://doi.org/10.1590/s1806-66902014000100005.

Santos, J.A., de Oliveira, K.F., da Silva Araújo, I.C., Avelino, I.I.F., de Sousa Cajuí, K.N., de Lacerda, L.D., Marins, R.V., 2016. Phosphorus partitioning in sediments from a tropical reservoir during a strong period of drought. Environ. Sci. Pollut. Res. 23, 24237–24247. https://doi.org/10.1007/s11356-016-7629-6.

Santos, J.A., Marins, R.V., Aguiar, J.E., Chalar, G., Silva, F.A.T.F., Lacerda, L.D., 2017. Hydrochemistry and trophic state change in a large reservoir in the Brazilian northeast region under intense drought conditions. J. Limnol. 76, 41–51. https://doi.org/10.4081/jlimnol.2016.1433.

Snortheim, C.A., Hanson, P.C., McMahon, K.D., Read, J.S., Carey, C.C., Dugan, H.A., 2017. Meteorological drivers of hypolimnetic anoxia in a eutrophic, north temperate lake. Ecol. Model. 343, 39–53. https://doi.org/10.1016/j.ecolmodel.2016.10.014.

Souza Filho, F.A., Martins, E., S P, R., Porto, M., 2006. The Mixing process in semiarid reservoirs and its implication on water quality. Rev Bras. Recur Hídricos 11 (4), 109–119 (in Portuguese).

Spears, B.M., Carvalho, L., Perkins, R., Kirika, A., Paterson, D.M., 2012. Long-term variation and regulation of internal phosphorus loading in Loch Leven. Hydrobiologia 681, 23–33. https://doi.org/10.1007/s10750-011-0921-z.

Sperling, M.V., 2007. Wastewater Characteristics, Treatment and Disposal. Iwa Publishing, New York, p. 292.

Stefanidis, K., Varlas, G., Vourka, A., Papadopoulos, A., Dimitriou, E., 2021. Delineating the relative contribution of climate related variables to chlorophyll-a and phytoplankton biomass in lakes using the ERA5-Land climate reanalysis data. Water Res. 196, 117053. https://doi.org/10.1016/j.watres.2021.117053.

Tammeorg, O., Möls, T., Niemistö, J., Holmroos, H., Horppila, J., 2017. The actual role of oxygen deficit in the linkage of the water quality and benthic phosphorus release: potential implications for lake restoration. Sci. Total Environ. 599, 732–738. https://doi.org/10.1016/j.scitotenv.2017.04.244. –600.

Tammeorg, O., Nürnberg, G., Niemistö, J., Haldna, M., Horppila, J., 2020. Internal phosphorus loading due to sediment anoxia in shallow areas: implications for lake aeration treatments. Aquat. Sci. 82, 1–10. https://doi.org/10.1007/s00027-020-00724-0.

Toledo, A.P.J., Talarico, M., Chinez, S.J., Agudo, E.G., 1983. The application of simplified models for the evaluation of the eutrophication process in tropical lakes and reservoirs. In: Brazilian Congress of Sanitary and Environmental Engineering, Santa Catarina. Brazilian Association of Sanitary and Environmental Engineering, pp. 1–34 (in portuguese).

Toné, A., Lima Neto, I., 2019. Simplified modeling of total phosphorus in Brazilian lakes and reservoirs. Rev. DAE 221, 142–156. https://doi.org/10.36659/dae.2020.012 (in portuguese).

Tong, Y., Liang, T., Wang, L., Li, K., 2017. Simulation on phosphorus release characteristics of Poyang Lake sediments under variable water levels and velocities. J. Geogr. Sci. 27, 697–710. https://doi.org/10.1007/s11442-017-1401-9.

Townsend, S.A., 1999. The seasonal pattern of dissolved oxygen, and hypolimnetic deoxygenation, in two tropical Australian reservoirs. Lakes Reservoirs Res. Manag. 4, 41–53. https://doi.org/10.1046/j.1440-1770.1999.00077.x.

Vollenweider, R.A., 1968. Water management research. Scientific fundamentals of the eutrophication of lakes and flowing waters with particular reference to nitrogen and phosphorus as factors in eutrophication. Organization for Economic Co-operation and De. Limnology and Oceanography 15, 169–170. https://doi.org/10.4319/lo.1970.15.1.0169.

Wang, J., Chen, J., Ding, S., Luo, J., Xu, Y., 2015. Effects of temperature on phosphorus release in sediments of Hongfeng Lake, southwest China: an experimental study using diffusive gradients in thin-films (DGT) technique. Environ. Earth Sci. 74, 5885–5894. https://doi.org/10.1007/s12665-015-4612-3.

Wang, M., Zhang, H., Du, C., Zhang, W., Shen, J., Yang, S., Yang, L., 2021. Spatiotemporal differences in phosphorus release potential of bloom-forming cyanobacteria in Lake Taihu. Environ. Pollut. 271, 116294. https://doi.org/10.1016/j.envpol.2020.116294.

Wiegand, M.C., do Nascimento, A.T.P., Costa, A.C., Lima Neto, I.E., 2021. Trophic state changes of semi-arid reservoirs as a function of the hydro-climatic variability. J. Arid Environ. 184, 104321. https://doi.org/10.1016/j.jaridenv.2020.104321.

Willmott, C.J., 1981. On the validation of models. Phys. Geogr. 2, 184–194.

Xu, Z., Yu, C., Sun, H., Yang, Z., 2020. The response of sediment phosphorus retention and release to reservoir operations: Numerical simulation and surrogate model development. J. Clean. Prod. 271, 122688. https://doi.org/10.1016/j.jclepro.2020.122688.

Yang, J., Lv, H., Yang, J., Liu, L., Yu, X., Chen, H., 2016. Decline in water level boosts cyanobacteria dominance in subtropical reservoirs. Sci. Total Environ. 557–558, 445–452. https://doi.org/10.1016/j.scitotenv.2016.03.094.

Zhang, H., Boegman, L., Scavia, D., Culver, D.A., 2016a. Spatial distributions of external and internal phosphorus loads in Lake Erie and their impacts on phytoplankton and water quality. J. Great Lake. Res. 42, 1212–1227. https://doi.org/10.1016/j.jglr.2016.09.005.

Zhang, Y., He, F., Liu, Z., Liu, B., Zhou, Q., Wu, Z., 2016b. Release characteristics of sediment phosphorus in all fractions of West Lake, Hang Zhou, China. Ecol. Eng. 95, 645–651. https://doi.org/10.1016/j.ecoleng.2016.06.014.

Zhang, W., Xu, Q., Wang, X., Hu, X., Wang, C., Pang, Y., Hu, Y., Zhao, Y., Zhao, X., 2017. Spatiotemporal Distribution of Eutrophication in Lake Tai as Affected by Wind. Water (Switzerland), vol. 9. https://doi.org/10.3390/w9030200.

Zhang, C., Yan, Q., Kuczyńska-Kippen, N., Gao, X., 2020. An Ensemble Kalman Filter approach to assess the effects of hydrological variability, water diversion, and meteorological forcing on the total phosphorus concentration in a shallow reservoir. Sci. Total Environ. 724 https://doi.org/10.1016/j.scitotenv.2020.138215.

Zheng, S. sha, Wang, P. fang, Wang, C., Hou, J., 2015. Sediment resuspension under action of wind in Taihu Lake, China. Int. J. Sediment Res. 30, 48–62. https://doi.org/10.1016/S1001-6279(15)60005-1.

Zhu, G., Yang, Y., 2018. Variation laws and release characteristics of phosphorus on surface sediment of Dongting Lake. Environ. Sci. Pollut. Res. 25, 12342–12351. https://doi.org/10.1007/s11356-018-1777-9.

Zou, R., Wu, Z., Zhao, L., Elser, J.J., Yu, Y., Chen, Y., Liu, Y., 2020. Seasonal algal blooms support sediment release of phosphorus via positive feedback in a eutrophic lake: Insights from a nutrient flux tracking modeling. Ecol. Model. 416, 108881. https://doi.org/10.1016/j.ecolmodel.2019.108881.